



Chair of Drilling and Completion Engineering

Master's Thesis



Continuous Drill String for Laboratory-
Scale Drilling Rig

Alexander Bazoev

September 2023



AFFIDAVIT

I declare on oath that I wrote this thesis independently, did not use other than the specified sources and aids, and did not otherwise use any unauthorized aids.

I declare that I have read, understood, and complied with the guidelines of the senate of the Montanuniversität Leoben for "Good Scientific Practice".

Furthermore, I declare that the electronic and printed version of the submitted thesis are identical, both, formally and with regard to content.

Date 18.09.2023

Signature Author
Alexander Bazoev

Alexander Bazojev
Master Thesis 2023
Petroleum Engineering

Continuous Drill String for Laboratory- Scale Drilling Rig

Supervisor: Univ.-Prof. Gerhard Thonhauser
Advisor: Dr.mont. Petr Vita

Chair of Drilling and Completion Engineering

Dedicated to my parents.

Acknowledgments

I express my sincere gratitude to the Department of Petroleum Engineering for the opportunity to study and write the thesis. Thanks to Petr Vita for supervising, ideas and leading thoughts that were embodied in the work. I also want to thank Professor Gelfgat for his advice and tremendous experience, both professional and life, which he willingly shared. In addition, thanks to Alexey Arkhipov for giving the direction of the thesis and assistance.

Special thanks to my friends with whom we overcame this stage.

Abstract

Laboratory-scale drilling rigs open the opportunities for conducting investigations and testing of new equipment and technologies. Since field experiments with the real-scale installations are quite difficult, dangerous and expensive, the miniature rigs provide useful alternatives for innovative researches of drilling processes and creation of modern devices.

The Montanuniversität MiniRig is one of the few of its kind and its development is an important goal of the department. The installation includes all the main systems inherent in industrial drilling rigs: rotary system, hoisting and circulation systems. The key advantage of the MiniRig is the control system which is presented by programmable logical controller (PLC). With the use of PLC automatic drilling operations are implemented, thus the prospects of full automation of drilling rigs can be investigated.

However, the current setup is not equipped with pipes hold and supply system. Therefore, it can't perform drill string connection operations in automatic regime to substitute manual work on pipes screwing. Such restrictions do not allow to fully implement experiments on automation and study of drilling processes.

To enhance the functionality of MiniRig the continuous drill pipe connection system was designed. First of all, all the necessary tasks that the system should conduct were defined. The system combines pipe holding and feeding mechanisms and makes possible making up and breaking out operations in automatic mode. The next step involved determining of the general appearance and building the mechanical components using SolidWorks CAD. Also the limitations due to laboratory conditions are taking into consideration. The designed concept integrates a setback and a pipe supplier and represents the rotating cylinder with channels for pipes. Since at each moment of time one of the retained pipes is on the well center, drilling and tripping are carried out through the cylinder. Moreover, the pipe holding mechanism is used not only inside the channels of the cylinder, but also as slips near the drill floor. For the purpose of substantiation of the selected design feasibility the calculations of the key mechanical parameters of each unit were conducted.

The outcome of the work is the model of the continuous drill pipe connection system which is accompanied by the main mechanical calculations. Next, the designed system will be built and automated.

Zusammenfassung

Bohranlagen im Labormaßstab eröffnen die Möglichkeit, Untersuchungen und Tests neuer Geräte und Technologien durchzuführen. Da Feldexperimente mit den Anlagen im realen Maßstab ziemlich schwierig, gefährlich und teuer sind, bieten die Miniaturanlagen nützliche Alternativen für innovative Forschungen von Bohrprozessen und die Schaffung moderner Geräte.

Die Montanuniversität MiniRig ist eine der wenigen ihrer Art und ihre Entwicklung ist ein wichtiges Ziel des Fachbereichs. Die Installation umfasst alle Hauptsysteme, die industriellen Bohrgeräten eigen sind: Drehsystem, Hebe- und Zirkulationssysteme. Der Hauptvorteil des MiniRig ist das Steuerungssystem, das von einer speicherprogrammierbaren logischen Steuerung (SPS) dargestellt wird. Mit dem Einsatz von SPS werden automatische Bohrvorgänge implementiert, wodurch die Aussichten auf eine vollständige Automatisierung von Bohrgeräten untersucht werden können.

Das aktuelle Setup ist jedoch nicht mit einem Rohrhalte- und Versorgungssystem ausgestattet. Daher kann es keine Bohrstrangverbindungsverfahren im automatischen Modus durchführen, um manuelle Arbeiten am Verschrauben von Rohren zu ersetzen. Solche Einschränkungen erlauben es nicht, Experimente zur Automatisierung und Untersuchung von Bohrprozessen vollständig durchzuführen.

Um die Funktionalität von MiniRig zu verbessern, wurde das kontinuierliche Bohrohrverbindungssystem entwickelt. Zunächst wurden alle notwendigen Aufgaben definiert, die das System ausführen soll. Das System kombiniert Rohrhalte- und Zuführmechanismen und ermöglicht das Auf- und Ausbrechen im automatischen Modus. Der nächste Schritt bestand darin, das allgemeine Erscheinungsbild zu bestimmen und die mechanischen Komponenten mit SolidWorks CAD zu bauen. Auch die Einschränkungen aufgrund von Laborbedingungen werden berücksichtigt. Das entworfene Konzept integriert einen Rückschlag und einen Rohrlieferanten und stellt den rotierenden Zylinder mit Kanälen für Rohre dar. Da sich zu jedem Zeitpunkt eines der gehaltenen Rohre in der Bohrlochmitte befindet, werden Bohren und Auslösen durch den Zylinder durchgeführt. Darüber hinaus wird der Rohrhaltemechanismus nicht nur innerhalb der Kanäle des Zylinders verwendet, sondern auch als Schlicker in der Nähe des Bohrbodens. Um die Machbarkeit des ausgewählten

Entwurfs zu belegen, wurden die Berechnungen der wichtigsten mechanischen Parameter jeder Einheit durchgeführt.

Das Ergebnis der Arbeit ist das Modell des kontinuierlichen Bohrr Rohrverbindungssystems, das von den wichtigsten mechanischen Berechnungen begleitet wird. Als nächstes wird das entworfene System gebaut und automatisiert.

Table of Contents

Chapter 1.....	9
1.1 Background and Context.....	9
1.2 Scope and Objectives.....	10
1.3 Achievements.....	10
1.4 Overview of Thesis.....	10
Chapter 2.....	13
2.1 Analysis of reasons and purposes of well construction automation.....	13
2.2 Automated drilling rigs review.....	15
Chapter 3.....	31
3.1 Montanuniversität MiniRig development history.....	31
3.2 Design of the drill pipe tripping and connection system.....	35
Chapter 4.....	41
4.1 Motors selection for the cylinder lifting and rotating.....	41
4.2 Selection of pipe holding device.....	49
4.3 Evaluation of pipe holding device.....	58
Chapter 5.....	61
5.1 Summary.....	61
5.2 Evaluation.....	61
5.3 Future work.....	62
References.....	63
References.....	63

Chapter 1

Introduction

1.1 Background and Context

Automated systems are becoming increasingly in demand in the well construction process. Development and introduction of robotic solutions to the drilling process provide better operational key productivity indicators (KPIs), enhance safety conditions on a rig, and are suitable for application in remote areas such as offshore.

At first, their usage reduces the duration of such routine and frequently repeated drilling operations as tripping. Performance of the rig personnel may differ from best practices and as a consequence invisible lost time (ILT) appears. Automation of operations leads to improvement of drilling cost efficiency.

Furthermore, tripping operations of the drill string and casing running implies heavy mechanical labor, in which a significant physical exertion falls on the drilling crew. This results in increased risks to the health and safety of personnel. In this case, applying robotic solutions will decrease occupational illnesses and accidents and provide less influence of human factors on the process. Complete drilling rig automation is a prospective and desirable purpose that enables fully unmanned drilling in which a person will be assigned the role of an operator controlling the process.

According to the report on the Drilling Systems Automation Roadmap (DSA) Roadmap, which represents a systematization of proposals for the implementation of advanced drilling automation solutions, the main direction of improvement should be the development of robotic equipment for drilling rigs (Wardt, 2019). Such systems require high precision and reliability to ensure compliance with safety and health requirements and accurate execution of

the drilling plan. Therefore, a laboratory-scale drilling rig is a convenient solution to carry out tests and experiments before exploitation on real fields.

The existing MiniRig in the university laboratory is automated and enables the execution of operations in automatic mode through the programmable logical controller (PLC). It consists of derrick, top drive, hoisting system, sensors, and circulation system. One of the main features of MiniRig is a sprocket and chain system that transforms the rotational motion of the servo motor into translational drill string running. However, it does not have a setback or pipe supply and connection system. Therefore, it is impossible to conduct investigations most comprehensively, recreating the real conditions on a drilling rig. Moreover, this weak point entails the necessity of manual labor for pipe screwing.

1.2 Scope and Objectives

The project discusses existing industrial and laboratory cases of drill pipes connection automation for the sake of suggestion the solution for MiniRig. The problem solution will accelerate the drilling process on MiniRig, reducing the time needed for slip-to-slip connection and eliminating person participation in operations.

The main purpose of the master thesis is to improve the existing laboratory scale drilling rig with continuous drill stand connection system and create its detailed description, principle of operation, design and suggestion of further automation.

1.3 Achievements

The concept of the pipe holding and connection mechanism was designed with the use of SolidWorks CAD. It can be divided into the following main units: rotational cylinder which retains the pipes, suspenders of the pipes inside the channels, slips placed close to the drilling floor and the lifting system for picking up the pipes from threaded connection. All the mechanisms were described and the required calculations which ensure the system feasibility were conducted.

1.4 Overview of Thesis

In the second chapter the literature review is presented, which discusses the necessity of automation of tripping operations in real-scale drilling rigs from the point of view of time savings and occupational health based on the relevant statistics and analytical approaches. Then, existing examples of automated drilling rigs, both industrial and laboratory scale, were considered in order to find and analyze the design features suitable for MiniRig.

The third chapter describes the general view of the continuous drill pipe connection system and mechanical principles of its operation. Moreover, the model build in SolidWorks CAD is demonstrated.

In the fourth chapter the calculations of such significant parameters as speed, torque and inertia of the motors and holding force of the suspenders are presented for the purpose of the proper equipment selection and providing the feasibility of mechanisms.

The fifth chapter indicates the main outcome of the thesis and further prospects of MiniRig development.

Chapter 2

Literature Review

2.1 Analysis of reasons and purposes of well construction automation

Many operations on the drilling floor are repetitive work. As a result a drilling crew repeatedly performs the same type of actions. For example, it performs screwing and unscrewing of drill pipes, running in and pulling out of the hole the drill string.

Different drilling crews have different productivity. Moreover, due to human factors, the crew cannot guarantee complete coincidence of repetitive drilling operations with the same speed and quality over time. Accidents and injuries are possible due to accumulated fatigue and other man-made causes.

In turn, robots have the advantage of being able to perform typical actions multiple times and identically. In addition, the correct setup and programming of the operation of robot makes it possible to expect a consistent level of quality in the operations.

Thus, robots provide a stable and predictable process. As an example, let's consider the drill pipe connection operations by different drilling crews. Figure 2.1 shows a plot of slip-to-slip connection time.

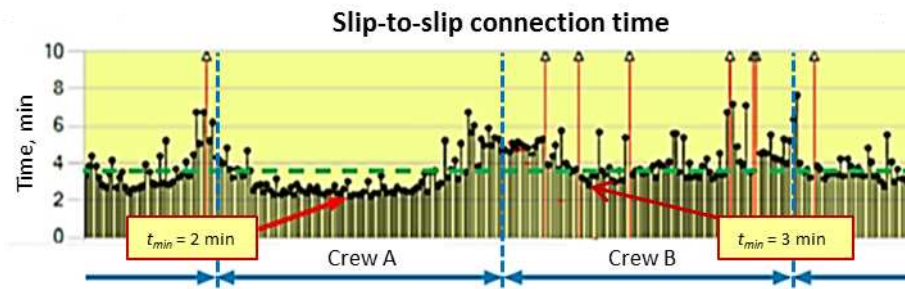


Figure 2.1 – Plot of time of drill string connection for different crews (Wijning, 2014)

As it is indicated, the minimum time spent on the operation by Crew A was about 2 minutes. This time is roughly indicative of the equipment's speed limit. From the assumption of complete repetitive operations at this speed, the tripping rate would reach about 3200 ft/h (975 m/h). However, it can be seen on the plot that Crew A was gradually increasing the speed during the initial interval of the work, then the time of performance was relatively constant, and by the end of the shift there was a decrease in productivity due to fatigue. It is also worth noting that the next drilling crew B was much slower, its best time was about 3 minutes. Overall, the average slip-to-slip connection time for the two crews was 3,5 minutes. Assuming the crews' actions were performed by the robot at a given speed equal to the best crew speed, it would have saved about 12 hours on tripping operations from a depth of 32000 ft (9754 m), which is equivalent to savings of \$500000.

Furthermore, it is important to note that the operations performed by a crew on a drilling floor are physically demanding and entail an increased risk of injuries. According to statistics from the International Association of Drilling Contractors (IADC), shown in Figure 2.2, tripping amounted to 21,29 % of all well construction incidents in 2021, the highest number of any type of operation. At the same time, making connection comprised 6,46 %.

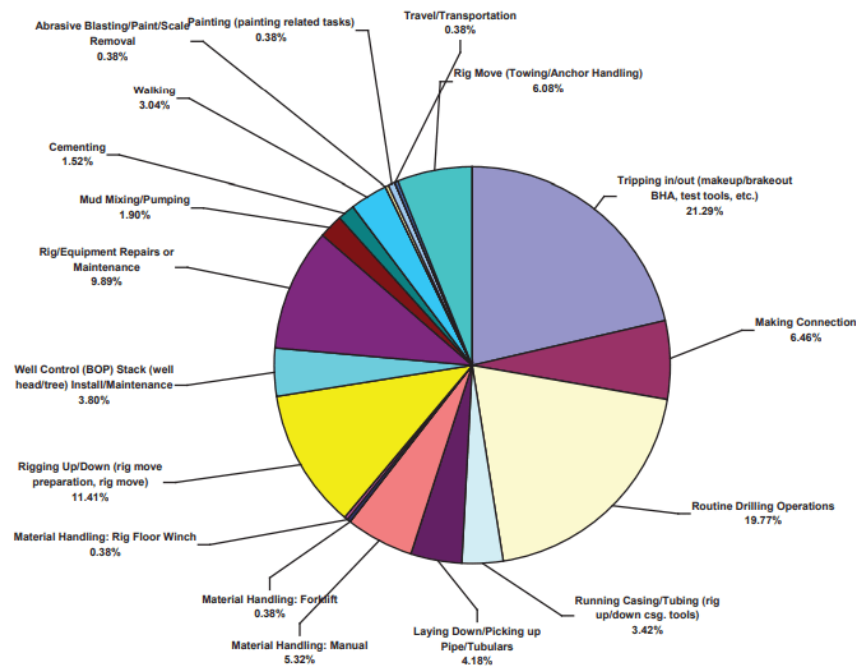


Figure 2.2 – Number of incidents during various drilling operations (IADC, 2022)

A similar ratio is observed when calculating total lost time in incidents: Tripping operations share is 25.00%, build-up amounts to 8.33%. Consequently, running in, pulling out and making pipe connections operations are the most unsafe during the process of well construction and require technological improvement. One of the solutions of this problem may be execution of such operations by robotic complexes and partial removal of personnel from dangerous zones.

As it can be seen, the identified factors have a significant impact on the duration and quality of the well construction and specify its further direction of improvement. Thus, the necessity of drilling process optimization determines the main goals of robotic complexes application:

- increasing the drilling speed by reducing time spent on routine technological operations such as drill string tripping and connection;
- reduction of non-productive time and invisible lost time by optimizing manual work of the crew;
- increasing of safety of technological operations by minimization of physical participation of personnel in dangerous works (Иванов et al., 2022).

2.2 Automated drilling rigs review

Throughout the history of the development of drilling technologies, attempts have been made to create automated systems to increase the productivity of well construction, unify the workflow and minimize the human factor. The main focus was on the pipe-handling

operations on the rig floor and the drill or casing string tripping process, because they are frequently repeated during the well construction (Boyadjieff, 1988).

In general, robotic drilling solutions can be classified into several groups. The most cutting-edge part is fully automated drilling rigs, usually consisting of a complex of several robots. The second one includes systems responsible for certain operations. In addition, it is possible to divide the systems into operating on real fields and laboratory versions.

The main achievements in the development of automated systems for the drill string connection and running will be described in this chapter.

2.2.1 Automated real-scale drilling rigs

In recent years, there has been competition in the field of drilling automation. However, the process of research and design, construction, testing and full-fledged commissioning takes many years of painstaking work and requires, among other things, expensive equipment and components. That is why, today there are not so many ready-made solutions for automated drilling, and even existing ones are still in the process of improving the technology (Rassenfoss, 2021).

2.2.1.1 Fully robotized drilling rigs

Full automation of drilling process implies the interaction and data exchange between different robots composing the complex. Thus, the unified system is achieved to perform all the steps of the well construction process in accordance with plan.

Since the mid of 1960s, attempts have been made to create the Automatic Drilling Machine (ADM), which scheme is shown in the Figure 2.3 (Boyadjieff, 1988). For this purpose experience and principles from machine-tool industry were adopted to update the drilling rig design. Hydraulic top-drive was used instead of rotary table. Tripping operations were conducted by hydraulic cylinders, which substitute drawworks. The transfer arm performed pipe movement from or to pipe racks and was capable to switch pipe position between vertical and horizontal. All drilling activities were carried out from a driller's cabin using pre-programmed automatic sequences. In total, within the framework of the project, 3 drilling rigs were built over 20 years, which drilled several wells. Although the project was a breakthrough, it was not widely recognized because of complexity both in terms of automation and mechanisms. However, this example shows the challenge of the robotic drilling rig implementation.

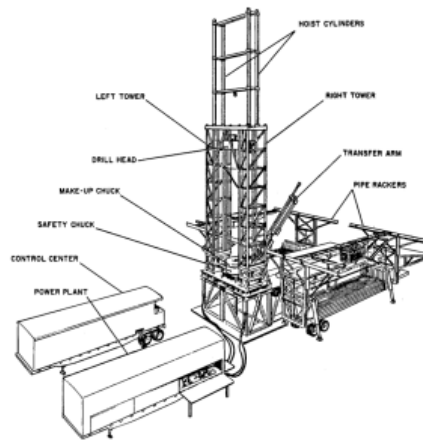


Figure 2.3 – Automatic drilling machine (ADM) (Boyadjieff, 1988)

In 1987, Rig-Automation Drilling (RA-D) project was started. It is capable to perform a diverse variety of drill floor operations with the help of the appropriate equipment: drawworks, top-drive, elevator, drill tongs, slips, pipe grabs. Controller is used to manage the processes in automated (handling and tripping of drilling instruments with diameter less than 20”) or in semiautomated mode (if more than 20”). The Figure 2.4 shows how these are arranged in the system.

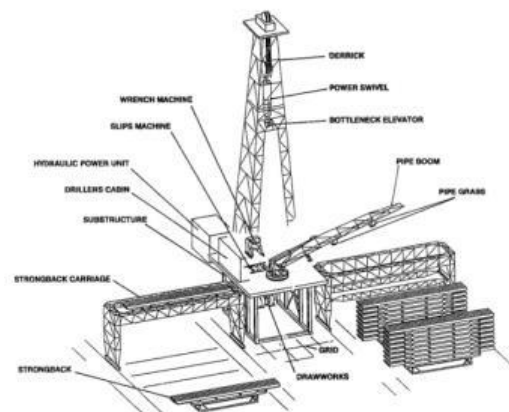


Figure 2.4 – Rig-Automation Drilling system (Simpson, 1992)

Another automation project was started by Robotic Drilling Systems AS in 2008 and since 2017 has been continued by Nabors. Nowadays, it is known that Nabors’ drilling rig called PaceR801 drilled the first well in October, 2021. The company states that its development is the first fully automated land rig in the world (Rassenfoss, 2021).

The robotic complex consists of four robots: Drill Floor Robot (DFR), Robotic Pipe Handler (RPH), Pipe Deck Handler (PDH), Robotic Roughneck (RRN), Multi-Size Elevator (MSE) (Cappuccio et al., 2019). The Drill Floor Robot, which is presented in the Figure 2.5, is a 6-axis robot capable to handle different BHA components by the spinning gripper.



Figure 2.5 – Drill Floor Robot (Cappuccio et al., 2019)

In the Figure 2.6 the Robotic Pipe Handler and Pipe Deck Handler are depicted. They are used for movement of drill pipes, casing, BHA components between setback and drill center, pipe racks and drill floor.



Figure 2.6 – Robotic Pipe Handler and Pipe Deck Handler (Raunholt et al., 2021)

Make-up and break-out operations are conducted by Robotic Roughneck, which is presented in the Figure 2.7. The main feature is the torque accuracy and ability to spin drill pipes, casings and subs.



Figure 2.7 – Robotic Roughneck (Raunholt et al., 2021)

Pipe handling is performed by Multi-Size Elevator which is shown in the Figure 2.8. It is powered hydraulically from the top-drive and is able to manipulate the objects with diverse sizes.



Figure 2.8 – Multi-Size Elevator (Cappuccio et al., 2019)

The Robotic Control System is responsible for the coordination between single robots, integrating them into one network, and allows to perform well construction operations in autonomous mode.

The results of experimental studies prove the efficiency of automated drilling system in comparison with manual work. It was defined that time savings for onshore rigs may reach 40 days in assumption of one year of operations. For offshore rigs potential savings are estimated at 38 days (Cappuccio et al., 2019).

2.2.1.2 Robots for pipe handling and tripping operations

In this section the separate robots for particular drilling activities are considered. In 2020, Huisman company suggested the system for automated drill string tripping and casing running operations, which is declared as the first in the industry (Mul et al., 2020). The authors tried to introduce the new approach for drilling rig selection in order to make the highest productivity the common goal both for operator, rig contractor and manufacturer. Therefore, they concentrated on reduction of time and cost per well instead of low rig day rates.

In order to accelerate rig up and rig down stages the mobile trailer platform for the drilling rig, which is noticeable in the Figure 2.9, was proposed. To provide a precise placement of the drilling rig in relation to the well center hydraulic racks were installed on the trailers, which are capable to manage the position. Application of the portable drilling rig allows to drill more wells within one field during the same time. While for the current rigs the full rig movement takes at least 17 hours, the considered system performs this procedure in 6 hours (Mul, 2020). Thereby, there becomes a potential for drilling 18 extra wells per year.



Figure 2.9 – Automated tripping operations system (Mul et al., 2020)

The system automatically handles pipes on the pipe racks, performing pipe caps removal, the pipe dope application and length measuring. Pipe handling unit is connected to the derrick trailer for the purpose of better positioning. Further, the pipe is moved to the well center by hydraulic pipe handler, where it is captured by automated hydraulic elevator in case of tripping operations. The hydraulic stabbing arm directs the pipe to the stick up in the rotary table and the wrench makes up the connection with the required torque value. Then, the hydraulic slips open and drill string with added pipe is ready to run in. The whole sequence of operations is automated and interconnected and parameters such as pipe length, torque, tripping rate are recorded and entered into the database. Similarly, the tripping out is performed.

Considering drill pipe connection while drilling, the principal distinction is that the pipe moved to well center attaches to the top drive, which screws it to the drill string without usage of tong.

In addition, the casing running automation technique differs only in the special casing running mechanism attached to the top drive and responsible for setting pipe into the stick up. The top drive rotates the casing and thus makes connection.

The results of the system testing show that tripping rate is more than 1800 ft/hr and 1400 ft/hr for drill string and casing correspondingly. Slip-to-slip stage during the automated pipe connection takes 85 sec that proves the prospects and efficiency of the process automation since the obtained time indicator is approximately 4 times less in comparison with an average field rig (Mul, 2020).

Completely different approach includes the usage of two hoisting systems in order to make pipe connections continually or nearly to it. The technology was proposed in Continuous Motion Rig (CMR) concept (Grinrod, 2010), Dual Multi-Purpose Tower (Roodenburg et al., 2017). According to Grinrod (2010), the continuous movement is enabled by mounting two lift systems in the derrick, which operate together sequentially as it is demonstrated in the Figure 2.10.

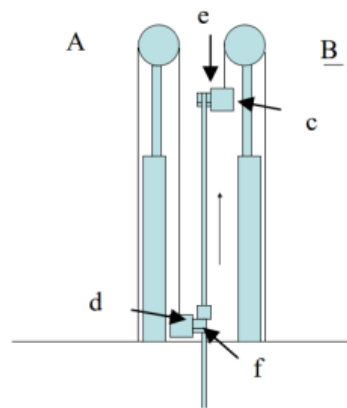


Figure 2.10 – Hoisting systems A and B, retractable tool holder c and d, tong and slips e and f (Grinrod, 2010)

Robots are programmed to perform operations both separately and parallel to each other. Their functionality represents rotation, vertical movement, retraction and extension of manipulator length. Such advantages of DMPT technology result in possibilities to manipulate 60 m stands, provide the tripping rate about 1700 m/hr and 70 sec for connection time (Grinrod and Krohn, 2011).

The process of tripping out and breaking out the drill string consists of the following operations. While one hoisting system is pulling the drill string out of the hole, another is moving upwards and simultaneously breaking down the pipe connection by means of the retractable tool holder and tong. When the pipe is released, the upper hoisting system opens its slips to allow tubular grabber pick it up from the well center, and the lower one is holding the remaining drill string. The upper hoisting system moves down, thus they switch the roles with the lower hoisting system and then the sequence is repeated.

The procedure of tripping in the drill string implies the particular sequence of actions presented in the Figure 2.11. At first, the tubular grabber supplies a new pipe from a setback to the well center, while the lower system implements drilling and circulation. Then, the new pipe is connected with the upper and lower hoisting systems.

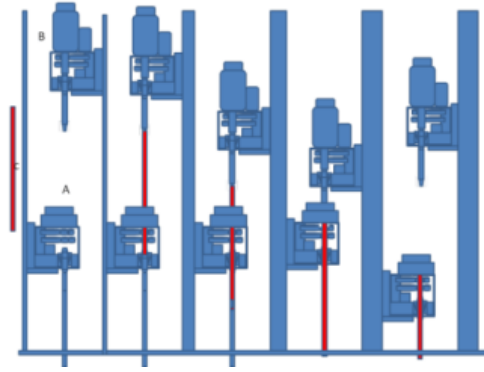


Figure 2.11 – Sequence of drill pipe connection (Skjaereth, 2014)

The upper system drills down with the new pipe. At the last step of the cycle the lower system disconnects the upper one from the drill string. While the upper system rises in order to receive a new pipe for making up, the lower system provides circulation and drilling.

Because of avoidance of the slip-to-slip connection time the rate of tripping operations increases significantly and are in the range 0,5-1 m/s or 1800-3600 m/hr. It is approximately equivalent to 60-120 30-meter stands per hour (Grinrod, 2010). In case of casing running the rate may reach 900 m/hr. It is stated that the aim of the project is to achieve time savings of 30-50% for one well. Until nowadays, the system has not been launched into commercial operation (Pilgrim and Butt, 2022).

Concerning DMPT construction, which is demonstrated in the Figure 2.12, it includes two hoisting systems and two cylindrical drums which play the role of rotational setbacks for pipe storage and supply. It enables to implement tripping operations and handling of drill pipes automatically at any height with the help of multifunctional robots, which are placed at each tower between the well center and drums. Two separate well centers allow to conduct multiple operations simultaneously and reduce the risk of occupational injuries.



Figure 2.12 – Manipulators of drill stands (Roodenburg et al., 2017)

Robots are programmed to perform operations both separately and parallel to each other. Their functionality represents rotation, vertical movement, retraction and extension of manipulator length. Such advantages of DMPT technology result in possibilities to manipulate 60 m drill stands, provide the tripping rate about 1700 m/hr and 70 sec for connection time.

2.2.2 Automated laboratory-scale drilling rigs

Development of miniature drilling rigs appears to be a useful approach for modeling of the real process. It is applied for the investigation of drill string behavior during drilling, evaluation of vibrations, testing of different BHA and, which is especially in focus, automation of the process.

The majority of existing laboratory rigs is mostly concentrated on studies of BHAs for directional drilling and autonomous measurement and control of drilling parameters and subsurface data. Nowadays, there is no solution for drill pipe connection automation. However, such drill floor operations also should be considered for the attainment of full automation of well construction process. Therefore, it is the prospective area of research for the organizations engaged in laboratory-scale rigs design. Nevertheless, it is necessary to discuss alternative laboratory rigs in order to note the design features which may be useful for MiniRig development.

It is worth mentioning that one of the stimulating factors is the Drillbotics competition, where universities present their results in construction of small drilling rigs. Conducted by SPE's Drilling Systems Automation Technical Section (DSATS), the contest is aimed at drilling process automation promotion. Student teams propose their solutions for designing of a miniature rig and an implementation of hands-free operations on it.

Generally, laboratory drilling rigs have the similar design consisting of the following main components, which to some extent replicate the real-scale ones: power system, hoisting system, rotary system, circulating system (Mitchell et al., 2011). Although the core functions have to be reproduced, the main difference from real size rigs lies in mechanical principles of system execution. It is explained by obvious requirements for compactness, size of the equipment. In order to identify the design features and operation principles, several examples of laboratory drilling rigs are analyzed.

2.2.2.1 Hoisting system

A hoisting system is necessary to provide lowering and rising of drill string. The design created by NTNU for Drillbotics competition is presented in the Figure 2.13.



Figure 2.13 – NTNU laboratory drilling rig (Lescoeur et al., 2017)

The suggested approach is represented by the ball screw drive. The concept, which is shown in the Figure 2.14, was selected instead of conventional drawworks for the purpose of simplification, higher precision, less friction and creation of the sufficient WOB, since the weight of drill string is not enough for the rock sample penetration.

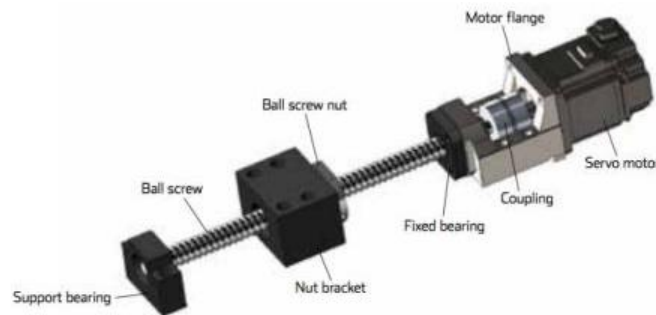


Figure 2.14 – Ball screw with servo motor (Lescoeur et al., 2017)

To drive the screw a helical geared motor is used (Mannsverk, 2019). The ball screw drive transfers rotational motion of the motor into linear motion of the ball screw nut, to which the platform with drill pipe is attached. In addition to ball screw, linear roller guides located on the side vertical racks ensure directional movement of the platform in one plane, rigidity of the system and stability of WOB measurements.

Another one solution was proposed by University of Stavanger, whose hoisting system includes three actuators with stepper motors and platform attached to them as it is seen in the Figure 2.15. Moreover, tri-axial load cells are mounted to each of the actuator to provide measurements of hook load and freely suspended weight.



Figure 2.15 – Hoisting system with stepper motors (Løken and Løkkevik, 2019)

It ensures the stability of position, vibration resistance, sufficient lifting force and allows for smaller incremental changes in WOB.

The idea of Oklahoma University was to use the pneumatic piston as a driver for the travelling block, which is depicted in the Figure 2.16. The unit consisting of motor, water swivel, torque sensor, RPM sensor and load cells is moving along the vertical axis on guide rails.

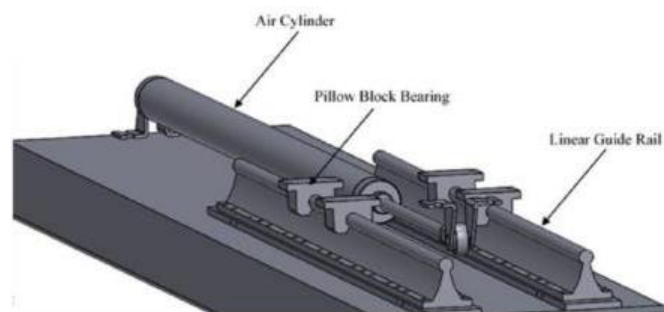


Figure 2.16 – Hoisting system with air cylinder (Akita et al., 2019)

2.2.2.2 Rotary system

The method of drilling influence a rotary system design and in some cases has changed over the years during the process of rig development and in dependence on the assigned tasks. Regarding the NTNU rig, a motor for top drive system was used to rotate the drill string in case of vertical well. To accomplish directional drilling, sliding mode is implemented. The entire drilling system is depicted in the Figure 2.17.

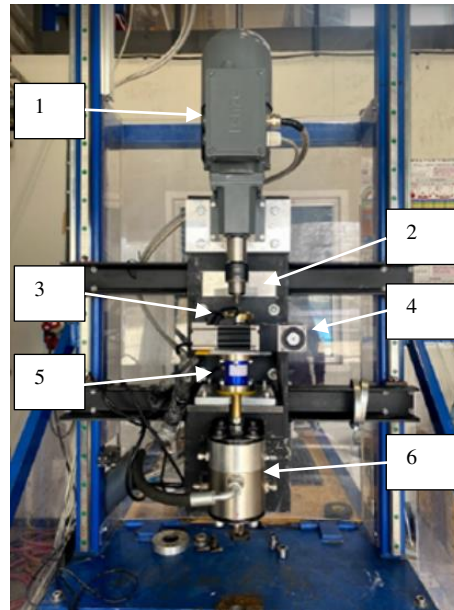


Figure 2.17 – Drilling system: 1– top drive, 2 – drill chuck, 3 – T-shaft, 4- azimuth motor, 5 – torque sensor, 6 – hydraulic swivel (Alvarez et al., 2022)

The top drive presented by helical geared motor creates a rotational movement of the drill bit separately from the entire drill string. The titanium rod which is located inside the drill pipe is used to transfer rotation. The drill string is sliding and can be rotated by azimuthal system. The rotary table is driven by azimuth servo motor connected with the hollow shaft gearbox which is applied to steer the drill string as it is shown in the Figure 2.18. The system rotation is transmitted to the drill string via T-shaft. Furthermore, for precise determination of torque the torque sensor is placed below the hollow shaft.

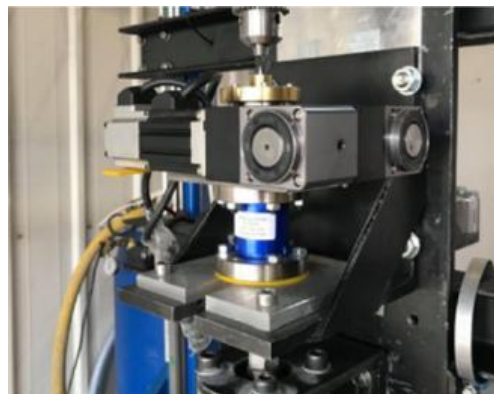


Figure 2.18 – Steering system (Alvarez et al., 2022)

The University of Stavanger minirig also has the combined system for both vertical and directional drilling. A hollow shaft brushless motor is used as top drive to rotate the drill string, set the toolface during drilling and keep angle in accordance with determined well path. For rotation of drill bit individually the downhole pneumatic motor is preferred rather

than electric because of its control simplicity via flow and pressure variation and smaller size while having comparable power.

Similarly, as it is demonstrated in the Figure 2.19, Oklahoma University also implemented the concept of torque transmission from the top drive downhole to the BHA through a stainless steel rod (cable) to remain drill pipe sliding.

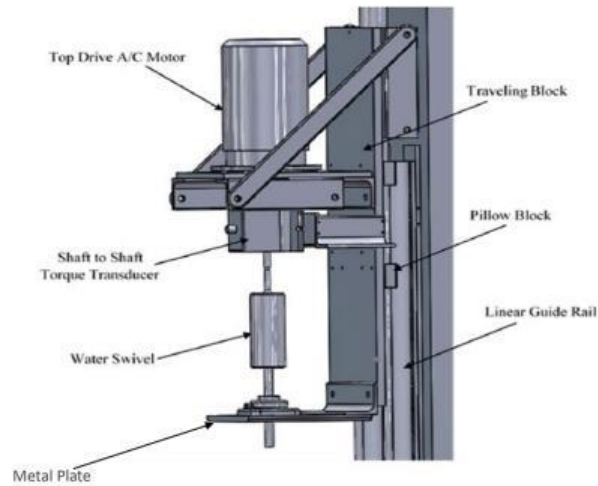


Figure 2.19 – Oklahoma University rig's top drive system (Akita et al., 2019)

2.2.2.3 Circulation system

In order to clean the well from drill cuttings, cool the bit and lubricate during drilling a circulation system is applied. In case of NTNU rig, the system presented in the Figure 2.20 include hydraulic swivel, located below the azimuth system, and diverter. The water plays the role of drilling mud and it is supplied through the hose and swivel to the drill string avoiding the drilling and azimuth systems. Diverter is used to provide a semi-closed loop system which more corresponds with HSE standard. The bell nipple and hose enables to divert the returned mud from the drill floor.



Figure 2.20 – Swivel and diverter (Alvarez et al., 2022)

Two different options of circulation systems are performed in the rig of Stavanger University, which operate individually in dependence with drilling trajectory. For vertical wells the conventional system is used including two alternating positive displacement pumps, as it is shown in Figure 2.21. Drilling mud passes through the hose attached to the swivel, hollow shaft motor, drill string and exits through the bit to the bucket.

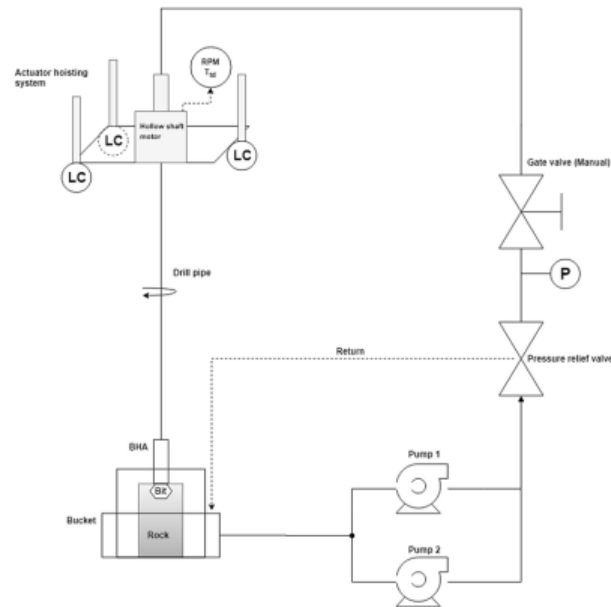


Figure 2.21 – Scheme of circulation system with two pumps (Khadisov et al., 2020)

A substantially different scheme of circulation is applied for directional drilling. Since the downhole pneumatic motor is used for bit rotation, the size of drill cuttings is very small resembling dust and can be easily transported into the air. To collect small particles, two vacuum cleaners are connected with collection box, as it is shown in the Figure 2.22.



Figure 2.22 – Collecting box of the pneumatic circulation system (Løken and Løkkevik, 2019)

In the circulation system of the University of Oklahoma drilling rig, the drilling mud is pumped from the tank through a polyvinyl chloride pipe to the travelling block, where it enters the drill string via a swivel. Then the mud passes through the drill string down to the bit, and then rises up through the annulus along with the cuttings. The cuttings are filtered out before the mud finally enters the circulation tank (Akita et al., 2019).

Chapter 3

MiniRig: development of the drill string tripping and connection system

3.1 Montanuniversität MiniRig development history

MiniRig represents an automated laboratory drilling rig created for the purpose of investigation of drill string behavior during drilling and the interconnection of different drilling parameters such as rotational velocity and WOB (Esmaeili et al., 2013).

3.1.1 Initial configuration

The first version of MiniRig, which is indicated in the Figure 3.1, was more similar with the real-scale installations in the operational principle than its successor.

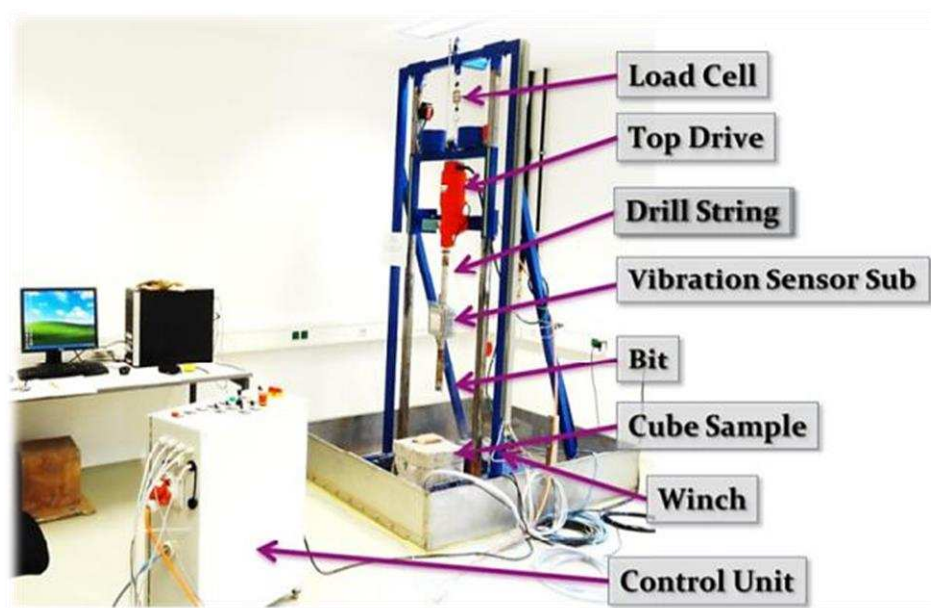


Figure 3.1 – First version of MiniRig (Esmaeili, 2013)

The derrick was represented by a steel frame with 2630 mm height, 1000 mm length and 800 mm width. It also includes two guide rails on which the travelling block with the attached top drive moves. The drill pipe was 524 mm length with outer and inner diameters 40 mm and 20 mm correspondingly, drill bit diameter – 2 and 2 3/8 inch.

Hoisting system involved drawworks, which composed by the servo motor driving the winch and regulating the ROP, pulley and drill line. Drill line is attached to the travelling block through the pulley. In addition, weights were applied to create a required WOB, since it is not possible to adjust the applied weight by drill collars and other components on the drill string in laboratory conditions. It was one of the drawbacks of the system, since the strength of the derrick imposes restrictions on the maximum weight.

Rotary system consisted of the top drive, which creates rotation of the drill string with adjustable speed, and a swivel for drilling fluid supply. Water plays the role of a drilling fluid and performs two functions simultaneously: cooling of the top drive motor and cleaning the wellbore from cuttings.

For measures of WOB of the top drive a load cell was attached to drill line between the travelling block and the frame. An ultrasonic sensor was connected to the travelling block and used to define the distance from it to the surface. With the help of the incremental encoder of the servo motor ROP and block position were measured. Restrictions of the top drive movements were provided by the means of safety sensors.

3.1.2 Current configuration

In the current version of MiniRig the hoisting system was modernized. Instead of the winch with the pulley and drill line, the drawworks are represented by the system of chain and sprockets, which drives the travelling block. Servo motor generates the motion of the system and sets the required WOB, when in the previous variant adding of weights was necessary. Gearbox is attached to the servo motor. Ratio between input and output torques can be defined using the formula:

$$G = \frac{\omega_1}{\omega_2} = \frac{T_2}{T_1}, \quad (1)$$

where G – gear ratio [-], $G = \frac{1}{48}$ in this case; ω_1, ω_2 – angular velocities of input and output gears respectively [RPM]; T_1, T_2 – input and output respectively [N·m].

Moreover, hoisting system renovation resulted in the derrick change as it is shown in the Figure 3.2. Now it is possible to drill below the floor to a depth about 3 m because of the opening bottom.

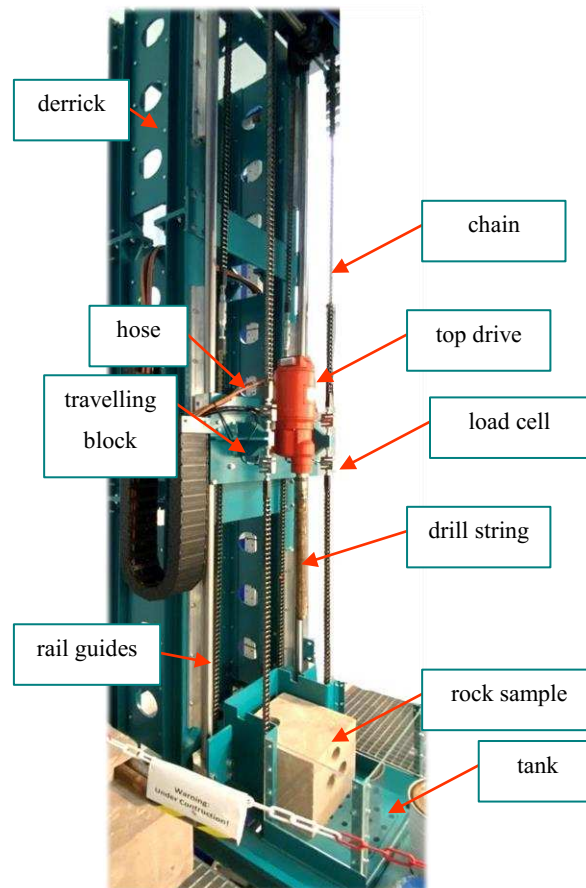


Figure 3.2 – Current version of MiniRig

Rotary system remains the same. The top drive motor, which is indicated in the Figure 3.3, is connected with a 3-stage gearbox. It allows to adjust the RPM between three values: 120, 240 and 360 RPM.



Figure 3.3 – MiniRig top drive

Nominal power is 5200 W and output power – 4000 W. The dependence between output torque T and other motor parameters is the following:

$$T = \frac{P}{2\pi \cdot n}, \quad (2)$$

where P – output power [W]; n – rotational speed [RPM].

As it was mentioned for the first setup, the top drive is connected with the circulation system through the hose. Minimum water flow rate is 1 l/min and the pressure is restricted by 3 bar. Water is supplied from the laboratory building water system and flows through the hose to the bit. A solenoid valve is used for adjusting of the water supply. Drilling cuttings are pumped out to the tank on the drilling floor (Aoun, 2023).

Regarding the sensors, four load cells are included into the chain of the hoisting system above and below the travelling block in order to measure hook load.

Four inductive proximity sensors are located in the well vertical axis. They detect and announce the appearance of metal objects in the sensing range to prevent the travelling block from going beyond the limits of safe operation.

Incremental encoder is placed on the shaft of the hoisting system. It implies for measurements of angular displacement of the shaft and further calculation of angular velocity.

The sensors are connected to the control unit which includes PLC for processing of parameters (Delmis, 2021). Adjustment of drilling process is provided via the remote console which is demonstrated in the Figure 3.4.



Figure 3.4 – Drilling console

The drilling data is transferred to the computer via Ethernet port (Aoun, 2023). Real-time drilling parameters are indicated on the special page of the computer monitor as it is depicted in the Figure 3.5.



Figure 3.5 – Page with drilling parameters

3.2 Design of the drill pipe tripping and connection system

The next stage of MiniRig development is the creation of automated system for feeding and screwing of drill pipes, which will minimize manual labor and reduce the slip-to-slip connection time.

The components of the drill pipe tripping and connection system should be a mechanism for feeding drill pipes to the well center, a setback holding the pipes, a drill wrench and slips. Several options of the system configuration are considered.

One of the concepts is a robotic manipulator located on a platform or suspended on the derrick, having several axes and capable of moving the pipe from the setback to the well center and back. In addition, the robotic manipulator is equipped with a multifunctional gripper capable of holding, screwing and unscrewing pipe connections. However, such a system is difficult to implement and expensive due to the large number of degrees of freedom.

The next option is to combine the functions of a setback and a feeding mechanism by installing a cylinder with longitudinal channels in which drill pipes are placed. The principle of operation is similar to a revolver drum, which implements the functions of a magazine and a chamber. The cylinder rotates around its axis, and at each moment of time one of the channels is located on the well center, thereby the running in and pulling out of the drill string are carried out through it.

The system should perform two types of motion:

- linear – to pick up the pipe from the threaded connection after unscrewing;
- rotational – to rotate the cylinder in order to place the pipe into the empty channel or took the new pipe.

The idea of using a hydraulic cylinder to lift the drum was considered. However, it was decided to reject this option due to the complexity of automating the device and connecting the liquid supply line.

To provide linear motion ball screw is used in which the nut is driven by the rotation of the screw connected to the servo motor. At the same time the screw remains stationary in the vertical plane, which explains the selection of this approach. The model of the system is constructed in SolidWorks. The front and side views are presented in the Figure 3.6.

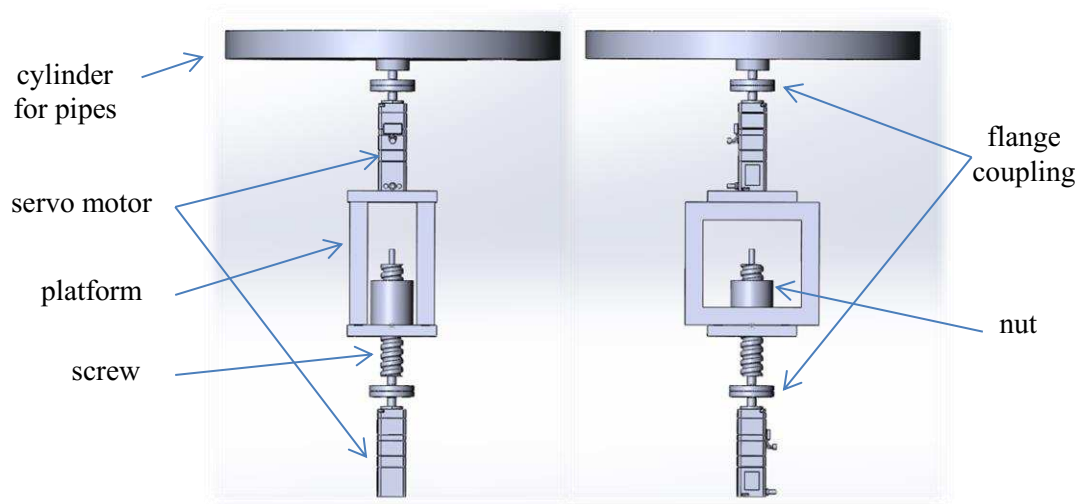


Figure 3.6 – Front and side views of the system

Since it is necessary to fix the system on the floor, the lifting system perceives the weight of the entire structure. The ball screw is convenient to apply because in this case the system is coaxial and only axial load occurs without bending stress. Also there is a restriction of the system's movement which means that the system cannot be below the anchorage level. For example, the rack and pinion mechanism is not suitable in this case, because at first, it is not coaxial: the lifting element is held only on the pinion resulting in bending stress. Secondly, the part of the rack equal to the lifting height of the system should initially be located lower than the pinion attached to the floor, which is not applicable. The similar limitation will be in case of suspension of the system and placing the lifting drive mechanism on top.

Servomotors should be equipped with brakes for the purpose of overcoming the axial loads when the system is stationary. Connection between shafts of servomotors and both the screw and cylinder with pipes is performed by flange couplings.

The platform with servomotor which rotates the cylinder with pipes is attached to the ball screw nut. The cutout in the center of the cylinder is designed to place the pipe holding devices in it. Another possible option is attaching of such devices on the top of the cylinder. The auxiliary views of the system are demonstrated in the Figure 3.7.

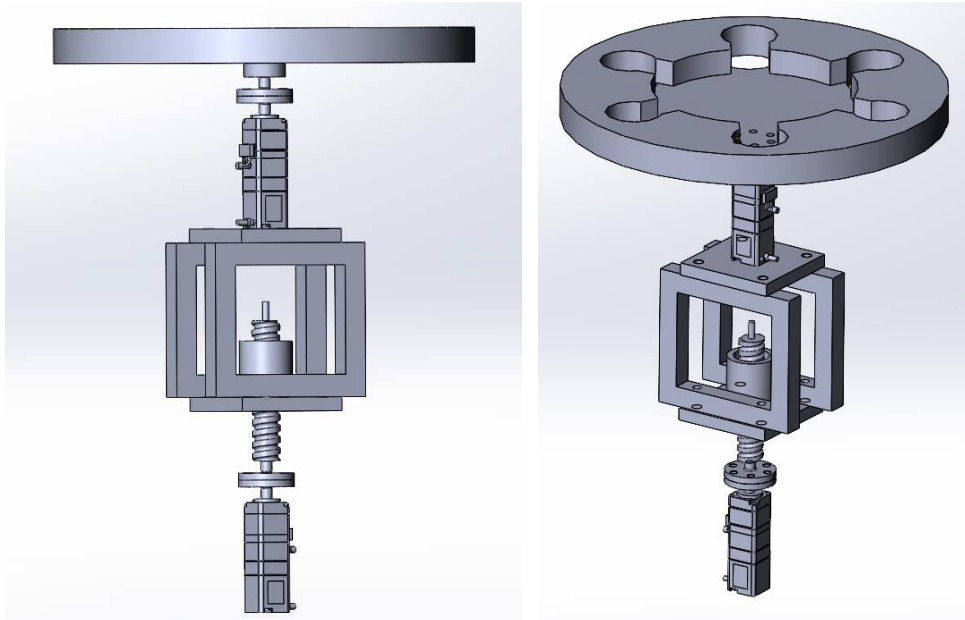


Figure 3.7 – Axonometric projection of the system

Since drill pipes should be retained in the channels, the holding system is required. One of the solutions for capturing pipes in channels is an electromagnetic lock. It holds the pipes inside the holes by magnetic interaction, when electricity is supplied, and releases the pipe, when the power is turned off. However, the presence of such a strong electromagnet can have an impact on the sensors located on the hoisting system, as well as in the drill string. In addition, non-magnetic drill pipes can also be used, which don't react to the magnet. In this regard, it is more appropriate to use gripping or suspending mechanism, which parameters will be defined in the next chapter.

Moreover, the drill string is usually suspended using the slips during the making up and breaking out the drill string connection on the surface. Because of the absence of the surface equipment on the drilling floor, the drill string runs and drills directly into the rock sample and there is no opportunity to insert the slips into the hole for suspension. Therefore, the mechanism similar to the pipes holding system for cylinder channels is suitable for performing the function of slips. The slips should be mounted on the drilling floor or on a platform that is fixed to the floor and rises slightly above it.

Figure 3.8 shows the sequence of operations for a drill pipe connection, which consists of the following steps:

1. The top drive descends to the new drill pipe located in the drum channel on the well center and screws on it.
2. The holding mechanism releases the pipe, the top drive with the attached new pipe descends to the drill string suspended on slips and screws on it.
3. Slips open and the drill string is run in.
4. The slips are closed, the top drive is unscrewed, it is lifted up, the drum is rotated by one division.

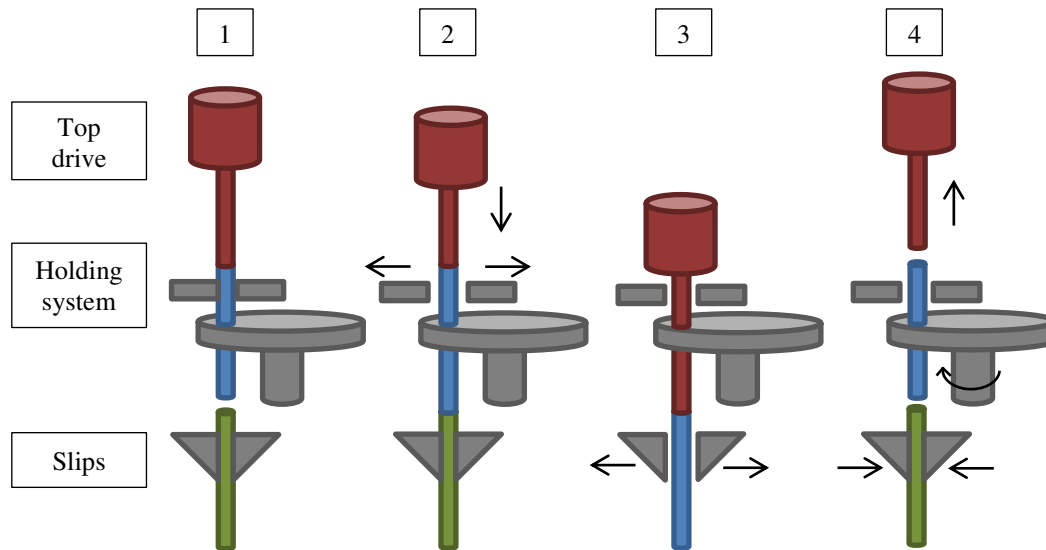


Figure 3.8 – Scheme of drill pipe connection

It can be noticed, that the joint pipe should be attached to the top drive in order to reach the drill string in the hole. It is necessary to provide the movement of the leading pipe and the top drive as a single unit and prevent mutual rotation between them. It means that they should be connected via coupling to transmit the top drive shaft rotation to the joint pipe and eliminate the mutual unscrewing during the pulling out of the drill string. In the scheme, the designation of the top drive implies a single system of the top drive and joint pipe.

Although the drill pipe connection is provided by the top drive rotation, the reverse process requires the presence of the drilling wrench for unscrewing. Since the current pipe is connected with top drive and the drill string, it is necessary to break out two connections during one cycle. It represents a separate mechanism installed on the drilling floor. The automated drilling wrench, better known in the industry as an iron roughneck, performs the functions of a drill pipe clamping and unscrewing. It consists of a support column and an arm which implements the assigned tasks. The arm is equipped with mechanism for clamping the pipe and spin-rollers which create the required torque. During the process of pipes break out the arm clamps the pipe and then the spinning rollers unscrew it.

When disconnecting pipes, the following sequence of actions is performed:

1. The drill string is lifted from the well and suspended on slips, the upper pipe is held by the holding system, the top drive unscrews from the drill string.
2. The top drive rises up, the drilling wrench unscrews the upper pipe.
3. The holding system captures the pipe, the cylinder is lifted up to remove the pipe from the threaded connection.
4. The cylinder is rotated by an empty channel on the well center, lowered to its original position.
5. The top drive descends to the drill string, screws onto it and rises up.

The scheme of disconnection operations is shown in Figure 3.9.

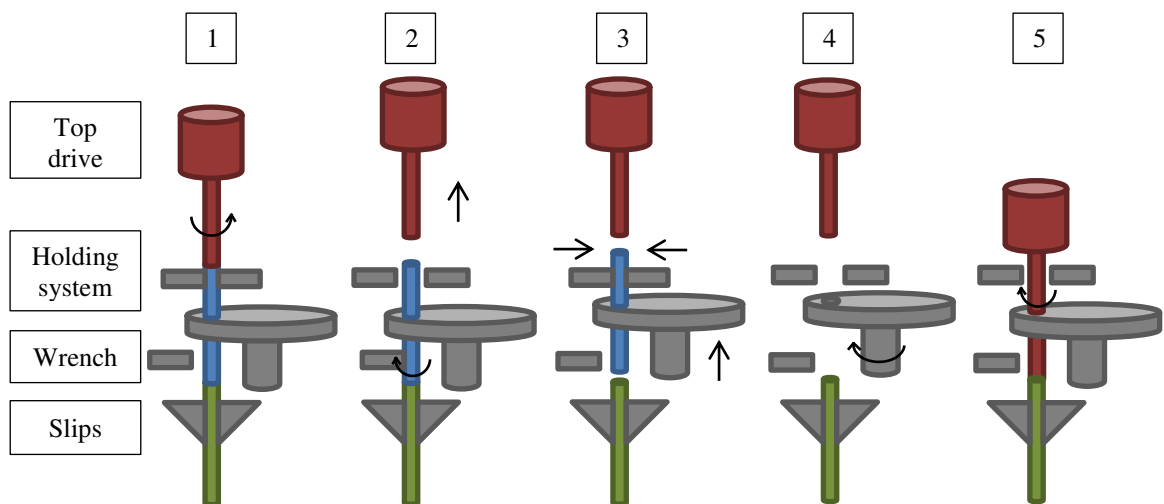


Figure 3.9 – Scheme of drill pipes breaking out

As the basis of a drilling wrench system, the development of Sha et al. (2022) presented in the Figure 3.10 can be adopted. The operation principle of the mechanism is the following. The piston rod of hydraulic cylinder is connected with the wedge plate and pushes towards the drill pipe. The follow-up rollers, which are attached to the wedge, clamp the drill pipe. Besides, the extension of the wedge plate drives the tangent wheels which are arranged symmetrically on its sides and belong to the near ends of the clamping arm. The wheels are bound by the spring in order to provide the return to the initial position when the load is removed. Since the clamping arm has an axis of rotation represented by a pin in its middle, the motion of the tangent wheels rotates the arm. As a result, the driving rollers placed on the far ends of the arm clamp the drill pipe. Thus, the drill pipe is pressed by four rollers. The required torque for unscrewing operations is created by the motors which actuates the driving rollers. The described combined mechanism for clamping and unscrewing provides the compactness of the system (Sha et al., 2022).

In order to eliminate the usage of hydraulic systems, a rack and pinion mechanism driven by a servo motor can be implemented instead of hydraulic cylinder with a piston.

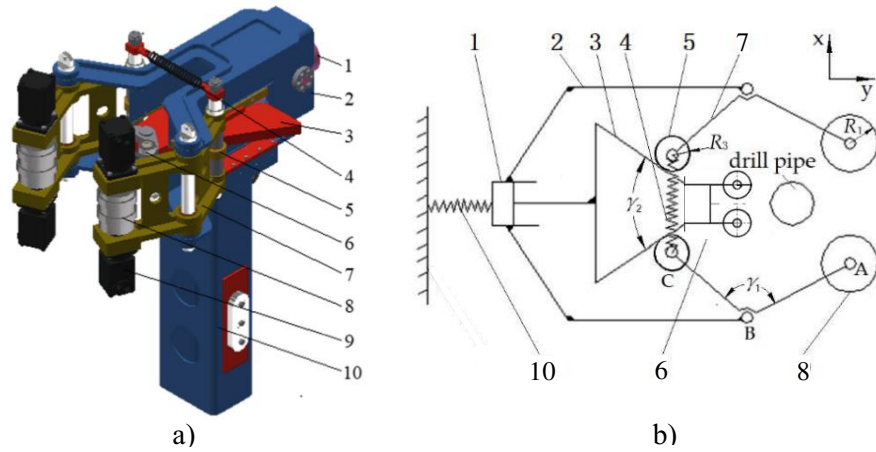


Figure 3.10 – Drilling wrench: a) model; b) kinematic scheme; 1 – hydraulic cylinder; 2 – cross beam; 3 – wedge plate; 4 – return spring; 5 – tangent wheel; 6 – follow-up roller, 7 – clamping arm, 8 – driving roller, 9 – hydraulic motor, 10 – upright column. (Sha et al., 2022)

The wrench is at fixed position and don't move on the drilling floor. Its arm is also at a fixed height below the cylinder. Therefore, when it is necessary to rotate the cylinder, it should be lifted above the level of the arm so that the pipes move freely without touching the wrench.

Chapter 4

Engineering calculations

4.1 Motors selection for the cylinder lifting and rotating

For determination of suitable motors it is necessary to evaluate the moment of inertia of the system, which indicates the resistance of the object to the rotational motion and depends on mass and geometry. Another important parameter is required torque, which characterizes the force needed to rotate the system.

4.1.1 Upper motor for rotation

4.1.1.1 Speed calculation

Operation process of the motor is divided into several phases: acceleration, work with a constant velocity, then deceleration and stopping. Let's set the values of time spent on acceleration t_a , deceleration t_d and time of stage with constant speed t_c :

$$\begin{aligned}t_a &= t_d = 0,1 \text{ [s]}, \\t_c &= 3 \text{ [s]}.\end{aligned}\tag{3}$$

Stop time t_s depends on the type and time of drilling activity: it can be drilling, running the drill string in or pulling out of the hole. Timing diagram of the motor's work which shows dependence between speed and time is shown in the Figure 4.1.

The angular velocity of the cylinder and motor's shaft is determined based on its definition and the number of carried pipes (sections of cylinder) is taken into account:

$$N_M = \frac{\Delta\varphi}{\Delta t} = \frac{\frac{2\pi}{N}}{t_o - 0} = \frac{\pi}{2} \cdot 60 = 29,452 \text{ [rpm]},\tag{4}$$

where $\Delta\varphi$ – angle of rotation [rad]; Δt – time interval when the rotation occurs [min]; N – number of pipes [pcs]; t_o – operation time [s].

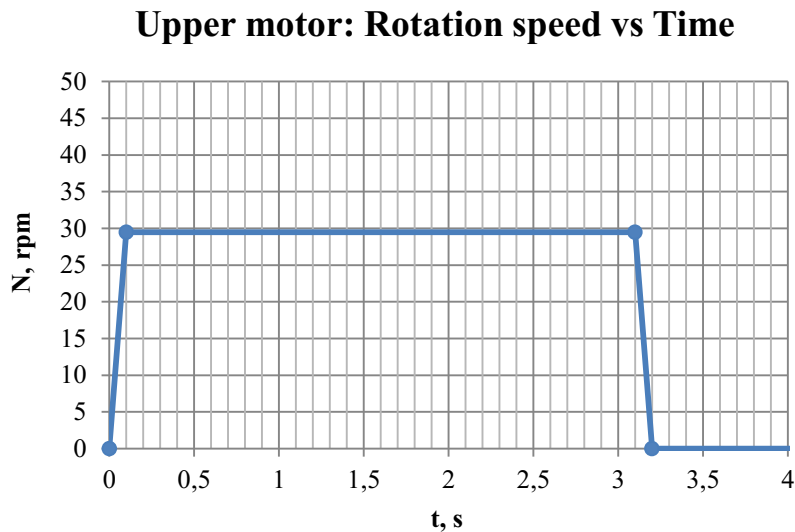


Figure 4.1 – Speed pattern of the upper motor

4.1.1.2 Moment of inertia calculation

The load acting on the motor consists of the cylinder, drill pipes and flange coupling. For the calculation of cylinder's inertia it was assumed as a solid cylinder:

$$J = \frac{1}{8}mD^2. \quad (5)$$

where m – mass of cylinder [kg]; D – diameter of cylinder [m].

Drill pipes shape can be approximately taken as a thick-walled cylinder and the following equation used:

$$J = \frac{1}{8}m(D^2 + d^2), \quad (6)$$

where m – mass of pipe [kg]; D, d – external and internal diameters of pipe [m].

Similarly the moment of inertia of flange couplings was defined.

Since the axis of the system's rotation is not the same with the pipe's one, Huygens–Steiner theorem was applied in order to determine the relationship between the appropriate moments of inertia:

$$J = J_c + mL^2, \quad (7)$$

where J_c – moment of inertia relative to the pipe's center of mass [$\text{kg}\cdot\text{m}^2$]; m – mass of pipe [kg]; L – distance between axes [m].

The required initial characteristics of components and results are reflected in the Table 4.1.

Table 4.1 – Results of moments of inertia calculation

Parameters	Cylinder	Pipes	Flange couplings
Outer diameter D [mm]	300	40	40
Inner diameter d [mm]	-	20	5
Length [mm]	5	530	27
Distance between axes L_a [mm]	0	70	0
Density ρ [kg/m^3]	2700	7830	7800
Number N [pcs]	1	4	1
Mass M [kg]	0,974	14,658	0,680
Moment of inertia J [$\text{kg}\cdot\text{m}^2$]	0,011	0,075	$1,960\cdot 10^{-5}$

Since moment of inertia is an additive parameter, for the complex object the total value is composed from inertia of its parts:

$$J_{total} = \sum_{i=1} J_i = 0,086 [\text{kg} \cdot \text{m}^2], \quad (8)$$

$$M_{total} = \sum_{i=1} M_i = 16,312 [\text{kg}], \quad (9)$$

where J_i – inertia of i^{th} component [$\text{kg}\cdot\text{m}^2$], M_i – mass of i^{th} component of the system [kg].

4.1.1.3 Torque calculation

Total torque consists of load and acceleration parts, which should be defined in order to choose the proper characteristics of motor. Load torque indicates the required amount of torque to overcome the gravitational and frictional components of load acting on the object. In turn, acceleration torque, which is also called inertia torque, appears on during acceleration or deceleration of the object.

Since the friction force is negligible, load torque can be assumed $T_L = 0$ [$\text{N}\cdot\text{m}$]. The motor is tentatively chosen taking into consideration that its permissible load inertia should be higher than $0,086 \text{ kg}\cdot\text{m}^2$. The servo motor NXM610M-PS25 (company – Oriental Motor), which is equipped with a gearhead with gear ratio $i = 25:1$, is a suitable option. Motor parameters we are interested in are indicated in the Table 4.2.

Table 4.2 – Selected motor parameters

Parameters	Values
Permissible load inertia J [kg·m ²]	0,091
Rotor inertia J ₀ [kg·m ²]	0,0334·10 ⁻⁴
Rated torque T _M [N·m]	6,44
Maximum instantaneous torque T _{MAX} [N·m]	19,3
Rated speed [rpm]	120
Gear ratio i [-]	25

Rotor inertia which is obtained from the selected motor specification influences the acceleration torque as it is noticeable from the formula:

$$\begin{aligned}
 T_a &= \frac{(J_0 \cdot i^2 + J_L) \cdot N_M}{9,55 \cdot t_a} = \frac{(J_0 \cdot i^2 + J_L) \cdot N_M}{9,55 \cdot t_a} = \\
 &= \frac{(0,0334 \cdot 10^{-4} \cdot 25^2 + 0,086) \cdot 29,452}{9,55 \cdot 0,1} = 2,724 \text{ [N} \cdot \text{m]},
 \end{aligned}
 \tag{10}$$

where J₀ – rotor inertia [kg·m²]; i – gear ratio [-].

By summing up the load and acceleration torque values total required torque is defined:

$$T = T_L + T_a = 0 + 2,724 = 2,724 \text{ [N} \cdot \text{m]}. \tag{11}$$

By comparison of the received value with rated torque of the selected motor T_M = 6,44 [N·m], we can conclude that it is within allowed range. Similarly to the speed pattern, dependence between torque and time is presented in the Figure 4.2.

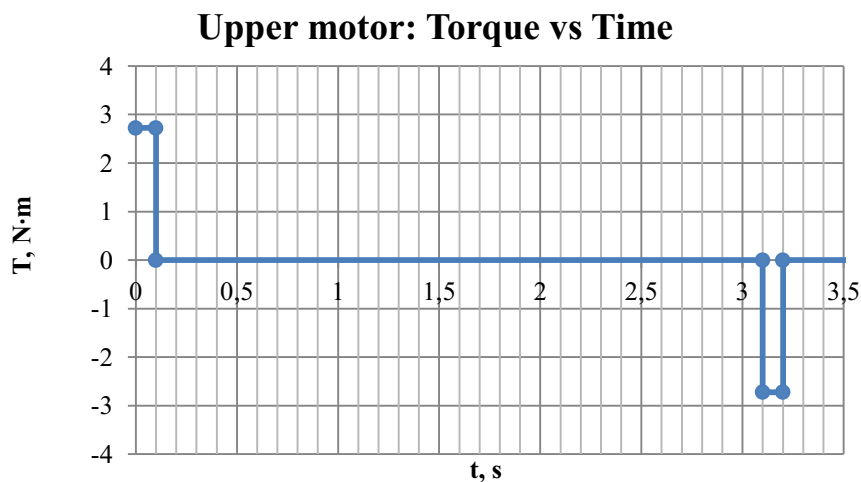


Figure 4.2 – Torque pattern of the upper motor

To define the effective load torque a root mean squared torque is calculated:

$$T_{rms} = \sqrt{\frac{(T_L + T_a)^2 \cdot t_a + T_L^2 \cdot t_o + (T_d - T_L)^2 \cdot t_d}{t}} =$$

$$= \sqrt{\frac{(0 + 2,724)^2 \cdot 0,1 + 0^2 \cdot 3 + (2,724 - 0)^2 \cdot 0,1}{3,2}} = 0,681 [N \cdot m]. \quad (12)$$

Then it is necessary to check that the following condition is met:

$$\frac{T_M}{T_{rms}} = \frac{6,44}{0,681} = 9,456 \geq S_f = 1,5 \quad (13)$$

4.1.2 Ground motor for linear movement

The ground motor should perceive the higher load. In addition to the load acting on the upper motor appears weight of this motor, platform where it is fixed, support beams, ball nut and ball screw.

4.1.2.1 Speed calculation

To obtain the rotary speed in RPM the linear velocity is converted using the equation:

$$N_M = \frac{V_L}{P_B}, \quad (14)$$

where V_L – linear speed [m/min]; P_B – lead of screw [m].

Taking into account that $V_L = 5$ [mm/s], we receive:

$$N_M = \frac{V_L}{P_B} = \frac{5 \cdot 60}{8} = 37,5 [rpm]. \quad (15)$$

The plot reflected in the Figure 4.3 describes the variation of speed during the motor work. The time for acceleration and deceleration is assumed equal – $t_a = t_d = 0,1$ [s], constant velocity phase time – $t_c = 2$ [s].

Lower motor: Rotation speed vs Time

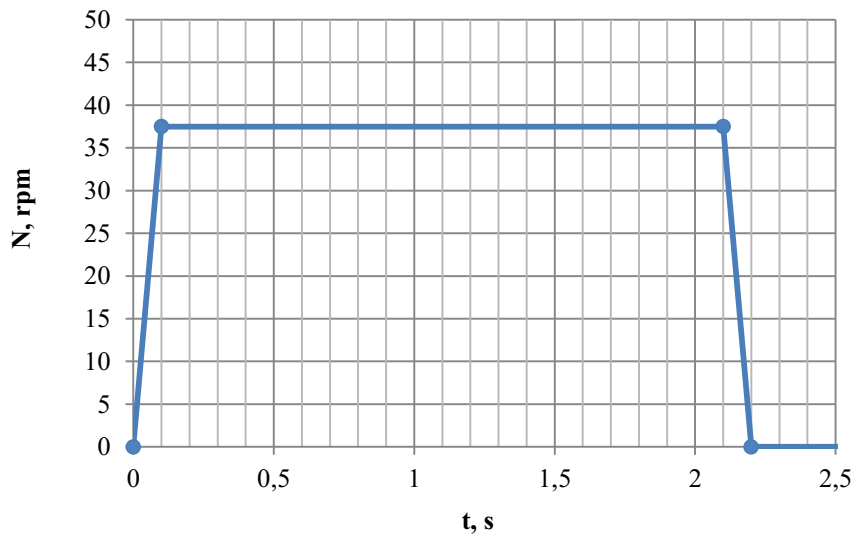


Figure 4.3 – Speed pattern of the lower motor

4.1.2.2 Moment of inertia calculation

Moment of inertia of the platform is calculated as a rectangular cuboid using the equation:

$$J = \frac{1}{12}m(a^2 + b^2), \quad (16)$$

Where m – mass of the platform [kg], a, b – length and width of cuboid [m].

Inertia of the upper motor which is placed on the platform also can be defined using the formula (16).

Support beams represent the tubes with square cross section, therefore they can be considered as four cuboids for the purpose of calculation simplification and formulas (16) and (7) are applied.

Ball nut include a cuboid shape platform with an opening in the center and a thick-walled cylinder. Therefore, the moment of inertia can be defined using equations (16), (6) and (7).

Moment of inertia of ball screw is calculated with the next formula:

$$J = \frac{1}{4}mD^2, \quad (17)$$

where m – mass of the screw [kg], D – diameter of screw [m].

The required parameters and results are reflected in the Table 4.3.

Table 4.3 – Results of moments of inertia calculation

Parameters	Platform	Support beams	Ball nut platform	Ball nut shaft	Ball screw
Length A [mm]	80	120	80	-	-
Width B [mm]	80	16	80	-	-
Height H [mm]	5	110	10	40	100
Thickness of walls S [mm]	-	16	-	-	-
Outer diameter D [mm]	-	-	-	38	20
Inner diameter d [mm]	-	-	-	20	-
Distance between axes L_a [mm]	0	30	0	0	0
Density ρ [kg/m ³]	2700	2700	2700	7800	7800
Number N [pcs]	1	2	1	1	1
Mass m [kg]	0,0864	0,547	0,173	0,032	0,245
Moment of inertia J [kg·m ²]	$9,216 \cdot 10^{-5}$	0,002	$9,216 \cdot 10^{-5}$	$7,371 \cdot 10^{-6}$	$1,225 \cdot 10^{-5}$

Total mass of elements comprising load to the lower motor is $M_{total} = 19,145$ [kg], total moment of inertia $J = 0,089$ [kg·m²].

4.1.2.3 Torque calculation

Axial force F of moving direction of the system can be generally derived from Newton's second law:

$$F = F_e + mg(\sin \theta + \mu \cos \theta), \quad (18)$$

where F_e – external force [N]; m – mass of system [kg]; g – gravity acceleration [m/s²]; μ – frictional coefficient [-]; θ – angle between the object and ground [°].

In the case under consideration $\theta = 90^\circ$ and there is no external force. That is why the equation above is transformed into:

$$F = mg. \quad (19)$$

Load torque is defined by the formula:

$$T_L = \frac{FP_B}{2\pi\eta} + \frac{\mu_0 F_0 P_B}{2\pi}, \quad (20)$$

where P_B – lead of screw [m]; $\eta = 0,85 \dots 0,95$ – efficiency of ball screw [-]; $\mu_0 = 0,1 \dots 0,3$ – friction coefficient of preload [-]; $F_0 \cong \frac{1}{3}F$ – preload [N].

To find rated load torque safety factor S_f [-] is applied:

$$T'_L = T_L \cdot S_f. \quad (21)$$

The required parameters and results are reflected in the Table 4.4.

Table 4.4 – Results of torque calculation

Parameters	Values
Lead of screw P_B [mm]	8
Efficiency of ball screw η [-]	0,9
Friction coefficient of preload μ_0 [-]	0,3
Composite force F [N]	187,625
Preload F_0 [N]	62,542
Load torque T_L [N·m]	0,289
Safety factor S_f [-]	1,5
Rated load torque T'_L [N·m]	0,434

Preliminary selection of the motor is based on load inertia $J = 0,088$ [kg·m²]. The servo motor NXM610M-PS25 (company – Oriental Motor) selected as the upper motor is also acceptable in case of lower motor because its permissible load inertia is 0,091 [kg·m²].

Putting the rotor inertia into the formula (10) we obtain acceleration torque:

$$\begin{aligned} T_a &= \frac{(J_0 \cdot i^2 + J_L) \cdot N_M}{9,55 \cdot t_a} = \frac{(J_0 \cdot i^2 + J_L) \cdot N_M}{9,55 \cdot t_a} = \\ &= \frac{(0,0334 \cdot 10^{-4} \cdot 25^2 + 0,089) \cdot 37,5}{9,55 \cdot 0,1} = 3,569 [N \cdot m], \end{aligned} \quad (22)$$

where J_0 – rotor inertia [kg·m²]; i – gear ratio [-].

Total required torque:

$$T = T_L + T_a = 0,289 + 3,569 = 3,859 [N \cdot m]. \quad (23)$$

It is allowed, since the rated torque of the selected motor is 6,44 [N·m]. As well as for the speed, torque changing over is reflected in the Figure 4.4.

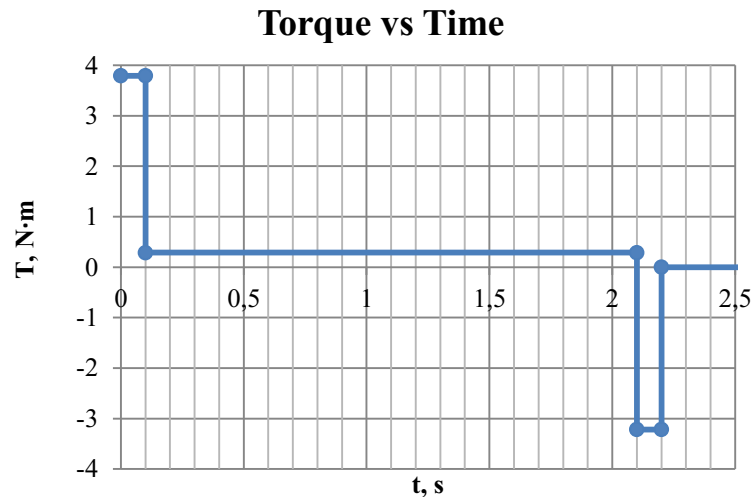


Figure 4.4 – Torque pattern of the lower motor

For the calculation of effective load torque equation (12) is applied:

$$\begin{aligned}
 T_{rms} &= \sqrt{\frac{(T_L + T_a)^2 \cdot t_a + T_L^2 \cdot t_o + (T_d - T_L)^2 \cdot t_d}{t}} = \\
 &= \sqrt{\frac{(0,289 + 3,569)^2 \cdot 0,1 + 0,289^2 \cdot 2 + (3,569 - 0,289)^2 \cdot 0,1}{2,2}} = \\
 &= 1,114 [N \cdot m].
 \end{aligned} \tag{24}$$

The effective load safety factor should be higher than 1,5-2. Since the rated torque is 5,98 times higher than effective load torque, the selected motor is permissible.

4.2 Selection of pipe holding device

During the well construction process the cylinder should keep the pipes inside channels and alternately release them when it is necessary to make connection or pick up while tripping out. In this section several options of the pipe gripping mechanism are discussed.

4.2.1 Pipe grippers

Grippers represent mechanisms for holding objects and are usually applied as executive devices of automated systems and are also known as end-of-arm tooling. Generally, they can be classified into several groups by the type of drive: vacuum, pneumatic, hydraulic and servo-electric (Suzuki and Shoyama, 2021). Advantages and disadvantages of each type are presented in the Table 4.5.

Vacuum grippers hold objects by suction which appears when the pressure is below than atmospheric. Such effect is provided by pumps which create continuous flow rate. This type

of grippers has particular requirements to the shape of objects to capture because suction cups should fit tightly to the surface. Moreover, the cleanliness of the environment is necessary for the smooth operation of the pump.

In case of pneumatic type compressed air is supplied through the pump or pressure line to drive the piston rod which is connected to grippers' fingers. The value of a gripping force depends on the pressure of air. The similar mechanism is implemented in hydraulic grippers. In this case hydraulic fluid is applied to move the piston instead of compressed air.

Electric approach means a usage of motors for creation motions of grippers' fingers. Servo motors provide control of a gripping process including the adjustment of a gripping force and position.

A mechanism of magnetic grippers usually doesn't imply the presence of fingers or other end-of-arm tools. Grabbing process is performed by a magnetic surface. It can either be a permanent magnet and no power supply is needed in this case or electromagnet driven by power supply.

Table 4.5 – Features of different types of grippers' drive sources

Type of power source	Advantages	Disadvantages
Vacuum	high flexibility, low cost	energy supply for pumps, high requirements to the dust content
Pneumatic	light weight, compactness, wide range of gripping force, low cost	compressed air supply line
Hydraulic	high gripping force	more efforts for cleaning and maintenance because of pumps and hydraulic fluid supply for them
Electric	wide range of gripping force, high flexibility, compactness	high cost
Magnetic	high gripping force, absence of fingers, low cost	additional device for disconnection of gripper in case of permanent magnet

Another one criteria for grippers classification is the type of end-of-arm tool:

- fingers, which can be parallel or angular and vary in number (usually 2 or 3);
- soft grippers, which fit an object and then grab it when air is pumped out;

- flat surface without fingers, especially used in magnetic type grippers;
- needle grippers, which pierce an object and move it.

Among all the types electric parallel grippers are mostly preferable from the automation point of view because they provide better control of parameters. Electric grippers consist of electric motor which is connected with the end effectors presented by fingers through the gear.

Although three fingers are potentially more suitable for grabbing a cylindrical object and allow more accurate alignment, in the case under consideration it is not possible to place the grabber above or under the pipe because it will block the axis of the well. Therefore, only lateral location is available and a gripper with two parallel fingers can be used.

The next step of gripper selection is calculation of the required gripping force to hold the pipe how it is shown in the Figure 4.5. Let's consider the simplified physical model of the process.

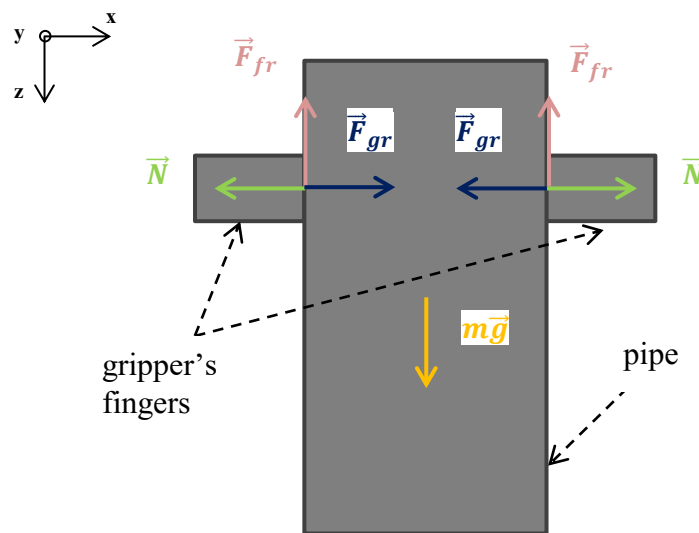


Figure 4.5 – Gripping scheme (side view)

Based on the 2nd and 3rd Newton's laws the equation describing the rest state of the system is obtained:

$$\begin{cases} 0 = mg - n \cdot F_{fr} \\ F_{fr} = \mu N \\ N = F_{gr} \end{cases}, \quad (25)$$

where F_{fr} – friction force [N]; N – reaction force [N]; $\mu = 0,35$ – friction coefficient between the aluminum gripper's finger and the steel pipe surface [-]; F_{gr} – gripping force [N]; $n = 2$ – number of fingers [-].

Using the received system of equations the grabbing force sufficient to balance the weight of pipe is divided:

$$F_{gr} \geq \frac{mg}{2\mu} = \frac{3,66443 \cdot 9,8}{2 \cdot 0,35} = 51,302 [N]. \quad (26)$$

Furthermore, the pipe is affected by torque of top drive that is schematically demonstrated in the Figure 4.6.

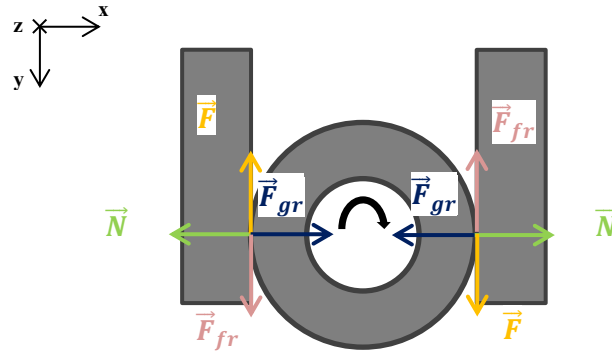


Figure 4.6 – Gripping scheme (top view)

To describe the equilibrium state of the system the following equations are applied:

$$\begin{cases} M = F \cdot r \\ 0 = F - F_{fr} \\ F_{fr} = \mu N \\ N = F_{gr} \end{cases} \quad (27)$$

where r – external radius of the pipe [mm].

Assuming that the maximum torque value is $M = 30 [N \cdot m]$ (Esmaeli, 2013) the value of gripping force should be:

$$F_{gr} \geq \frac{M}{r \cdot \mu} = \frac{3,66443}{20 \cdot 10^{-3} \cdot 0,35} = 4285,714 [N]. \quad (28)$$

4.2.2 Pipe suspender and new configuration of pipes

As soon as the gripping mechanism is provided mainly by the friction between the pipe and gripping fingers, it requires quite high gripping force generated by electric motor. Alternative options for pipes holding inside the cylinder's channels can be the suspending mechanism. For its implementation the pipes should be slightly modified. The new configuration implies the addition of grooves to the pipe walls, in which the latches enters. The principal scheme of the interaction between the pipe and suspender is presented in the Figure 4.7.

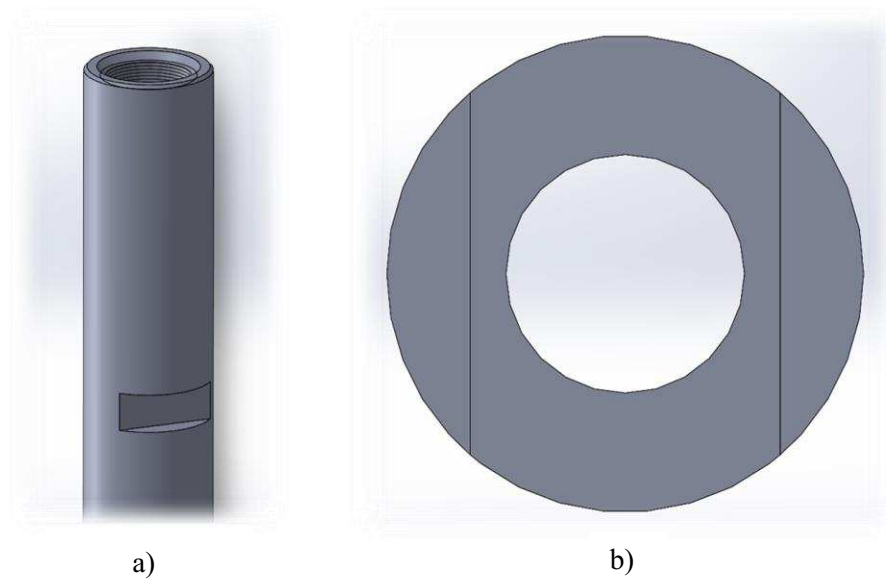


Figure 4.7 – Pipe with two grooves: a) axonometric projection; b) cross section of grooves

The possible option of the locking device represents the electromechanical mechanism which is demonstrated in the Figure 4.8. It consists of the retractable latch connected through the system of levers and spring with a cored solenoid. When the power supply is applied to the solenoid, a magnetic field is generated that draws in the core. It leads to compression of the spring and movement of the levers that push the bolt into the groove of the pipe. When the power is turned off, the core is pushed out by the action of spring and returns the bolt to its initial place releasing the pipe.

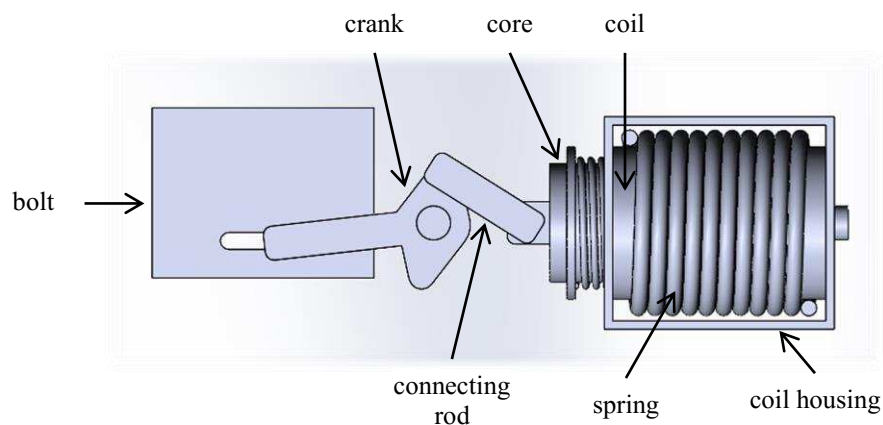


Figure 4.8 – Latch mechanism

Due to the similarity of the lever system with a crank mechanism, a part with a fixed axis of rotation can be conditionally called a crank, and the element connecting it to the core is a connecting rod. The bolt is inserted into housing which has special slot for the implementation of sliding mechanism. The crank is connected with the bolt by slider, thereby providing a linear movement.

Considering the interaction of the pipe and suspender, it is worth noting that the entire weight of the pipe will be applied to the latches. The load on one latch depending on their total number n can be calculated as follows:

$$F = \frac{mg}{n} = \frac{3,66443 \cdot 9,8}{2} = 17,956 \text{ [N]}. \quad (29)$$

In addition to gravity force, torque from the top drive also acts on the pipes during screwing and unscrewing as it is shown in the Figure 4.9.

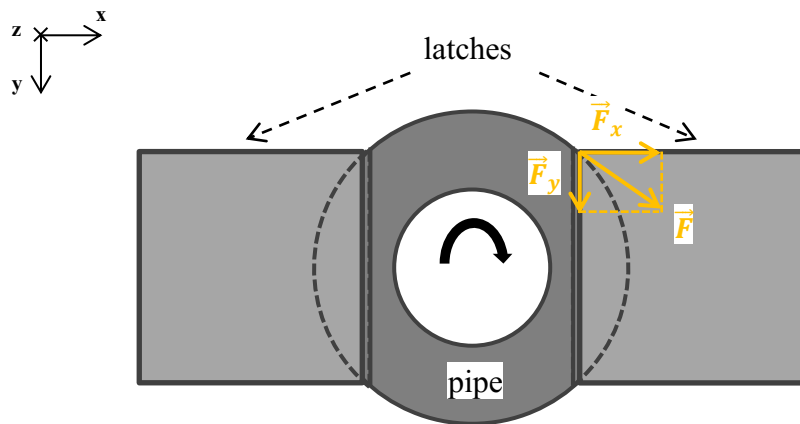


Figure 4.9 – Suspending scheme (top view)

The force which provides the torque is tangentially applied to the pipe and creates the load on the latch:

$$F = \frac{M}{r} = \frac{30}{20 \cdot 10^{-3}} = 1500 \text{ [N]}. \quad (30)$$

This load can be decomposed to axes X and Y. The angle between the force and its projection on the x axis is defined using the depth of the groove which is set $l_{groove} = 7 \text{ [mm]}$:

$$\alpha = \text{asin}\left(\frac{r - l_{groove}}{r}\right) = \text{asin}\left(\frac{20 - 7}{20}\right) = 40,542^\circ. \quad (31)$$

Then the values of forces projections can be calculated:

$$\begin{aligned} F_x &= F \cdot \cos \alpha = 1500 \cdot \cos(40,542^\circ) = 1139,901 \text{ [N]}, \\ F_y &= F \cdot \sin \alpha = 1500 \cdot \sin(40,542^\circ) = 975,000 \text{ [N]}. \end{aligned} \quad (32)$$

Considering the bolt in such conditions as a cantilevered beam bending loads in directions Y and Z and compression in X-axis are acting on it.

To define the force from solenoid which holds the core and correspondingly

In order to determine the force of the solenoid that draws the core and, accordingly, holds the bolt, it is necessary to differentiate the energy E_L by coordinate x of core's position (Schimpf, 2013):

$$F = \frac{dE_L}{dx} = \frac{I^2}{2} \cdot \frac{dL(x)}{dx}, \quad (33)$$

where L – inductance [H]; I – current through the coil [A].

For the purpose of approximate evaluation of solenoid force, the simplified formula can be used (Impulse Automation Ltd, 2017):

$$F = \frac{I^2 N^2 \mu_0 A}{2S_L^2}, \quad (34)$$

where N – number of coil turns [-]; A – cross-section of the coil [m²]; S_L – air gap between the core and the edge of coil [m]; μ_0 – air permeability [N/A²].

Suspending mechanisms should be fixed radially on the top of the cylinder surface so that the latches are diametrically opposite each other relative to the channel

The market analogue of such a mechanism is a household electromechanical lock of the solenoid type. As an example, consider the lock YB-500A of Ybi Electronics, indicated in the Figure 4.10.



Figure 4.10 – Example of the electromechanical lock (Shenzhen YLI Electric Lock Co.,Ltd., 2014)

It is made entirely of stainless steel, the declared by the manufacturer weight is 0,68 kg and holding force is 1000 kg or 9800 N. The shape of the bolt is cylindrical which is not as preferable as cuboid one applied in the case in question. Nevertheless, such a lock can be used as a ready-made template for further modification and programming for an existing task.

4.2.3 Slips for the drill string

The latches may perform the functions of slips in the case in question on the analogy of suspenders inside cylinder. It is worth mentioning that the difference between slips and pipe suspenders discussed in the previous chapter is the retained load. Since the drill string is

composed of several pipes, the weight which acts on the vertical direction is higher at times. Multiplying the equation (5) by $n_{pipes} = 4$ pipes in the drill string:

$$F = \frac{n_{pipes} \cdot mg}{n_{latches}} = \frac{4 \cdot 3,66443 \cdot 9,8}{4} = 35,911 \text{ [N]}. \quad (35)$$

Loads on other axes will not change because the torque is the same. To resist to the increased weight more latches can be required and for this purpose the following scheme of placing shown in the Figure 4.11 can be implemented.

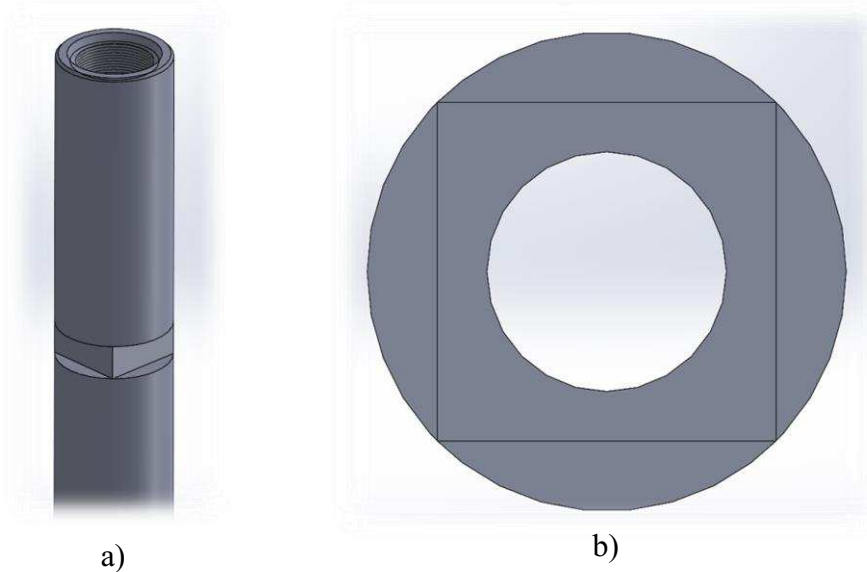


Figure 4.11 – Pipe with four grooves: a) axonometric projection; b) cross section of grooves

It means that instead of two grooves, as it was suggested for suspenders, four grooves are made in the pipe. It allows to apply four latches for drill string suspending. Nevertheless, in case of pipes in channels the suspending scheme will not change significantly since four grooves are symmetrically arranged on the pipe surface and two bolts can still be used.

4.2.4 Sensors of the pipe orientation

In order to hold or release the pipe the latches should precisely get into the grooves on the pipe. That is why it is important to control the position of the pipes and for such reason sensors are necessary to be installed. Since the arrangement of the grooves is symmetrical with respect to the transverse axis of the pipe, it is sufficient to set only one sensor opposite one of the channel grooves for correct pipe locking. Such sensors should be placed both on the cylinder with pipes and on the slips. Considering that the cylinder contains several channels for pipes, the position monitoring is required for each of them. However, to avoid installation of a large number of sensors, it is possible to set one sensor near to the well axis, which will

obtain the position of each pipe alternately when the cylinder rotates without reference to a specific channel.

When choosing a sensor, it should be taken into account that the pipes are in the process of movement and rotation, therefore the optimal option is a proximity type. According to the principle of operation, proximity sensors include capacitive, inductive, optical, ultrasonic kinds. They are based on change of electric field, capacitor capacity, magnetic field, light or sound waves propagation. Since the task is to recognize the position of the groove on the pipe, and not to detect the entire object, the most suitable methods are optical and ultrasonic.

Optical sensors are divided to several main types:

- through-beam sensor – based on the light flux from the transmitter to the receiver. It actuates when an object appears between them and interrupts the light flux;
- reflective – based on the reflection of the light beam from the reflector, with the transmitter and receiver located at the same point and the reflector opposite them. It is activated when the light flux is interrupted by an object;
- diffusive – similar with reflective, but the light beam is reflected from the object itself;

The diffusive type is the most applicable of them because it combines transmitter and receiver in one housing and does not require a reflector. To identify the side of the pipe where the groove is located, a contrasting photometric eyemark should be placed above or below the groove, from which the beam of light will be reflected. Figure 4.12 shows that the light beam bounced from the eyemark is recognized by the receiver as a target. Thus, it becomes possible to stop the rotation of the pipe so that the groove stands clearly opposite the bolt. It is recommended to use white eyemark in case of dark-colored surface of the object.

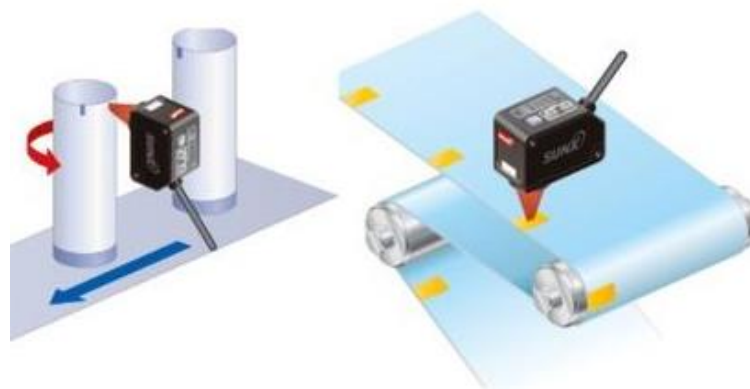


Figure 4.12 – Eyemark optical sensor (Panasonic Electric Works SUNX Co., Ltd., 2011)

Another option of optical sensors is laser rangefinder. Time of flight technology is based on the measurement of the time needed the laser pulse to travel from transmitter to the object and back to receiver. The distance is then determined using the measured time and velocity of light. Since the groove is deepened, the distance to it is greater than to the pipe surface. Thus by comparison of the distances, the target value can be set while programming the sensor. Another approach, which is presented in the Figure 4.13, relies on the measurement of phase shift between emitted and reflected flux and then calculating of the distance. Such technology is more accurate and cost efficient then the time of flight method.

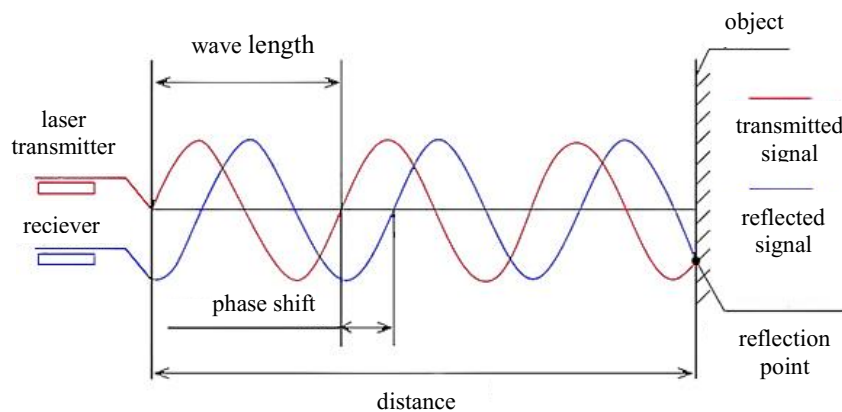


Figure 4.13 – Phase shift principle of laser rangefinder (Wang et al., 2020)

Regarding the ultrasonic sensors, the operation mechanism is the following: transmitter sends an ultrasonic wave with a frequency from tens to hundreds Hz directed toward the object, wave reflects from it and returns entering the receiver. By the measured time of the wave's path the distance to the object can be determined. The principle of sensor setting for groove recognition is similar with laser sensors and bases on the different distances to the groove and to the pipe surface.

4.3 Evaluation of pipe holding device

For the purpose of ensuring the drilling pipe is clamped with the drilling wrench, it is necessary to calculate the force acting from the wedge plate driven by the motor. In the Figure 4.14 the scheme of the system loading is presented to analyze the interaction of components.

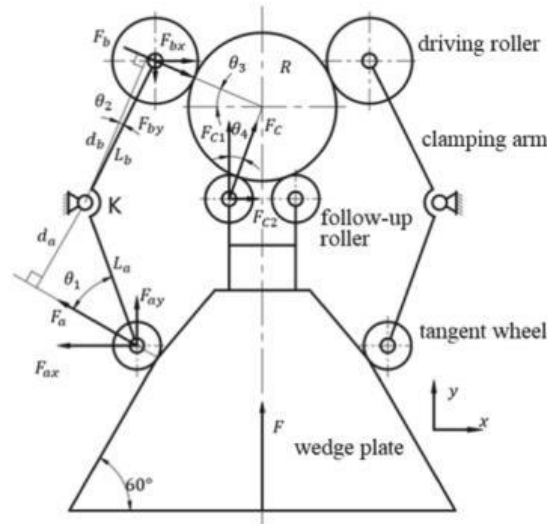


Figure 4.14 – Diagram of forces acting on the system (Sha et al., 2023)

Based on the formulas provided by Sha et al. (2023), the following equation for calculation of the clamping force F is derived:

$$F = \frac{M_{max}}{\mu R} \cdot \left(\sin \theta_3 + \frac{L_b \cos \theta_2}{2 \cdot L_a \sin \theta_1} \right), \quad (36)$$

where M_{max} – maximum torque of the spinner mechanism [N·m]; μ – coefficient of friction between the drill pipe and rollers [-]; R – radius of the drill pipe [m]; L_a, L_b – lengths of the clamping arm parts [m]; $\theta_1, \theta_2, \theta_3$ – angles reflected in the diagram [°].

Assuming the mentioned values as they are shown in Table 4.6, the clamping force is approximately evaluated.

Table 4.6 – Calculation of the clamping force

Parameter	Value
Maximum torque M_{max} [N·m]	30
Coefficient of friction μ [-]	0,2
Radius of the drill pipe R [m]	0,02
Length of the near part of arm L_a [m]	0,064
Length of the far part of arm L_b [m]	0,0664
θ_1 [°]	40,77
θ_2 [°]	0,91
θ_3 [°]	26,15
Clamping force F [N]	8839,67

Chapter 5

Conclusion

5.1 Summary

The master thesis discusses the prospects of the MiniRig development. The actual configuration of the laboratory-scale drilling rig provides the manual drill string connection and disconnection operations. It means that the current setup has no setback for pipes storage, slips for a drill string suspension and drilling tongs or iron roughneck for making up and breaking out. The analysis of existing laboratory rigs of other scientific organizations revealed that there are no ready-made solutions of such mechanisms. Therefore, the system for pipe supply and connection was designed.

The proposed version was based on the considerations of compactness and the feasibility in laboratory conditions due to restrictions of the space and equipment. That is why it represents not a reduced copy of existing field-scale inventions, but the original design solutions. The suggested system incorporates the functions of a setback, drill tongs and slips. The revolver cylinder principle with pipes inside the channels is taken as a mechanical basis of the pipe hold and supply system. Specially designed suspenders keep the pipes until one of them is on the well center when the cylinder rotates.

5.2 Evaluation

The project of MiniRig improvement was justified by the mechanical principles and calculations of the key components parameters. Therefore, the required speed, torque and moments of inertia of the servo motors were determined. In addition, the configuration of pipe suspending devices and control sensors were selected and the sufficient holding forces were defined. During the development of each unit of the system, several options for the implementation were discussed and substantiated. The designed drill pipe connection

mechanism provides the new techniques of the MiniRig operation since no manual labour is required for pipe screwing. It allows to conduct experiments with longer drill string than by the current installation. Furthermore, it becomes possible to implement the well construction operations in a more realistic way and more similar to the field drilling rig.

5.3 Future work

Further work implies the construction, making up and commissioning of the designed system. For the sake of MiniRig automation, inclusion of the new equipment into the unified control system and programming will become an essential part of the setting. The servo motors and pipe position sensors should be adjusted properly in order to provide the control of the operations through the programmable logical controller.

References

References

Akita, E., Dyer, F., Payton Duggan, Drummond, S. and Elkins, M. (2019) 'Design Report OU - Drillbotics™ 2019 Phase I'.

Alvarez, L., Helgeland, H., Ness, J. and Solberg Mikaela (2022) 'Design Report NTNU-Drillbotics® 2022 Phase I'.

Aoun, H. (2023) *MiniRig: Load Cells Array*, Master's thesis, Montanuniversitaet Leoben.

Boyadjieff, G. I. (1988) 'The Application of Robotics to the Drilling Process', *All Days*. Dallas, Texas, 2/28/1988 - 3/2/1988, SPE.

Cappuccio, P., Burrafato, S., Maliardi, A., Ricci Maccarini, G., Taccori, D., Dalla Costa, R., Raunholt, L. and Larsen, Ø. (2019) 'Full Robotic Drill Floor as Advanced Rig Automation', *Day 4 Thu, November 14, 2019*. Abu Dhabi, UAE, 11/11/2019 - 11/14/2019, SPE.

Delmis, K. (2021) *Laboratory Scale Drilling Rig*, Master's thesis, Montanuniversitaet Leoben.

Esmaeili, A. (2013) *Analysis of Drill String Dynamic Behavior*, Doctoral, Montanuniversitaet Leoben.

Esmaeili, A., Elahifar, B., Fruhwirth, R. K. and Thonhauser, G. (2013) 'Formation Prediction Model based on Drill String Vibration Measurements Using Laboratory Scale Rig', *All Days*. Dubai, UAE, 10/7/2013 - 10/9/2013, SPE.

Grinrod, M. (2010) 'Continuous Motion Rig: A Step Change in Drilling Equipment', *All Days*. New Orleans, Louisiana, USA, 2/2/2010 - 2/4/2010, SPE.

Grinrød, M. and Krohn, H. (2011) ‘Continuous Motion Rig. A Detailed Study of a 750 Ton Capacity, 3600 m/hr Trip Speed Rig’, *All Days*. Amsterdam, The Netherlands, 3/1/2011 - 3/3/2011, SPE.

IADC (2022) *IADC ISP Program 2021: Summary of Occupational Incidents (US Land Totals)*, IADC [Online]. Available at <https://www.iadc.org/wp-content/uploads/2022/07/2021-ISP-Annual-Report-for-US-Land-Totals.pdf>.

Impulse Automation Ltd (2017) *Linear Solenoid Technical Notes* [Online].

Khadisov, M., Hagen, H., Jakobsen, A. and Sui, D. (2020) ‘Developments and experimental tests on a laboratory-scale drilling automation system’, *Journal of Petroleum Exploration and Production Technology*, vol. 10, no. 2, pp. 605–621.

Lescoeur, A., Olsen, M. A., Vasantharajan, M. and Egeland, R. L. (2017) *Design and Construction of an Autonomous, Miniature Drilling Rig - Contribution to the Drillbotics™ Competition 2017*, Master thesis, Norwegian University of Science and Technology.

Løken, E. A. and Løkkevik, J. (2019) *Optimization of an Intelligent Autonomous Drilling Rig: Testing and Implementation of Machine Learning and Control Algorithms for Formation Classification, Downhole Vibrations Management and Directional Drilling*, Master, Stavanger, University of Stavanger.

Mannsverk, J. e. a. (2019) ‘Design Report NTNU - Drillbotics™ 2020 Phase I.’.

Mitchell, R. F., Miska, S. and Aadnøy, B. S. (2011) *Fundamentals of drilling engineering*, Richardson, TX, Society of Petroleum Engineers.

Mul, A. de (2020) ‘Full Automated Casing Running: The Next Step Completed in Field Automation’, *Day 3 Wed, November 11, 2020*. Abu Dhabi, UAE, 11/9/2020 - 11/12/2020, SPE.

Mul, A. de, Hooft, D. and Ziatdinov, S. (2020) ‘Step Changing Safety and Efficiency Gains by Fast Rig Moves, Automated Sequences and Data Processing’, *Day 2 Wed, March 04, 2020*. Galveston, Texas, USA, 3/3/2020 - 3/5/2020, SPE.

Panasonic Electric Works SUNX Co., Ltd. (2011) *Digital Mark Sensor LX-100 Series* [Online].

Pilgrim, R. and Butt, S. (2022) ‘Mitigating Surge and Swab by Changing Tripping from a Batch to a Continuous Process’, *Day 2 Thu, March 17, 2022*. Calgary, Alberta, Canada, 3/16/2022 - 3/17/2022, SPE.

- Rassenfoss, S. (2021) 'Drilling Automation - A Robot Takes Over the Drilling Floor', *Journal of Petroleum Technology*, vol. 73, no. 12, pp. 18–22.
- Raunholt, L., Meissner, S. and Kverneland, O. G. J. (2021) 'Field Experience from Robot Tests on Drill Floor and Pipe Deck', *Day 2 Tue, November 16, 2021*. Abu Dhabi, UAE, 11/15/2021 - 11/18/2021, SPE.
- Roodenburg, D., Andresen, J. A. and Huisman, M. Z. (2017) 'Full Scale Test Tower: Validation Real World Performance of Pioneering Drilling Efficiencies', *Day 1 Wed, April 05, 2017*. Bergen, Norway, 05.04.2017 - 05.04.2017, SPE.
- Schimpf, P. (2013) 'A Detailed Explanation of Solenoid Force', *Int. J. on Recent Trends in Engineering and Technology*, vol. 8, no. 2.
- Sha, Y., Li, Q. and Zhao, X. (2022) 'Study on the Position Deviation between the Iron Roughneck's Spin-Rollers and the Drilling Tool', *Applied Sciences*, vol. 12, no. 12, p. 5827.
- Sha, Y., Li, Q. and Zhao, X. (2023) 'Analysis of Mechanical Properties of Iron Roughneck's Spin-Rollers', in Yan, L. and Na, J. (eds) *PROCEEDINGS OF THE INTERNATIONAL CONFERENCE OF FLUID POWER AND MECHATRONIC [S.I.]*, ATLANTIS PRESS, pp. 393–404.
- Shenzhen YLI Electric Lock Co.,Ltd. (2014) *YB-500A(LED)* [Online].
- Simpson, B. K. (1992) 'Field Trials of the First RA-D (Rig Automation-Drilling) Automated Drilling Rig', *All Days*. New Orleans, Louisiana, 2/18/1992 - 2/21/1992, SPE.
- Skjaereth, O. B. (2014) 'Continuous Motion Rig (CMR Technology) - A Step Change In Drilling Efficiency', *All Days*. Kuala Lumpur, Malaysia, 3/25/2014 - 3/28/2014, OTC.
- Suzuki, K. and Shoyama, N. (2021) *Features and Functions of the EH Series Electric Gripper* [Online].
- Wang, Q., Tan, Y. and Mei, Z. (2020) 'Computational Methods of Acquisition and Processing of 3D Point Cloud Data for Construction Applications', *Archives of Computational Methods in Engineering*, vol. 27, no. 2, pp. 479–499.
- Wardt, J. P. de (2019) *Drilling Systems Automation Roadmap Report 2019-2025* [Online]. Available at <https://dsaroadmap.org/wp-content/uploads/2019/06/1-0f-14-Overview-Exec-Summary-190531.pdf>.
- Wijning, D. (2014) 'A New Approach On Automation Of Drilling Equipment', *All Days*. Bergen, Norway, 4/2/2014 - 4/2/2014, SPE.

Иванов, Б. В., Архипов, А. И. and Стесин С. Б. (2022) 'Обзор существующих роботизированных комплексов и технологических решений для морского бурения на арктическом шельфе', *Бурение и нефть*, no. 3.

List of Figures

Figure 2.1 – Plot of time of drill string connection for different crews (Wijning, 2014)	14
Figure 2.2 – Number of incidents during various drilling operations (IADC, 2022)	15
Figure 2.3 – Automatic drilling machine (ADM) (Boyadjieff, 1988)	17
Figure 2.4 – Rig-Automation Drilling system (Simpson, 1992).....	17
Figure 2.5 – Drill Floor Robot (Cappuccio et al., 2019).....	18
Figure 2.6 – Robotic Pipe Handler and Pipe Deck Handler (Raunholt et al., 2021)	18
Figure 2.7 – Robotic Roughneck (Raunholt et al., 2021)	18
Figure 2.8 – Multi-Size Elevator (Cappuccio et al., 2019)	19
Figure 2.9 – Automated tripping operations system (Mul et al., 2020)	20
Figure 2.10 – Hoisting systems A and B, retractable tool holder c and d, tong and slips e and f (Grinrod, 2010)	21
Figure 2.11 – Sequence of drill pipe connection (Skjaereth, 2014)	22
Figure 2.12 – Manipulators of drill stands (Roodenburg et al., 2017).....	22
Figure 2.13 – NTNU laboratory drilling rig (Lescoeur et al., 2017)	24
Figure 2.14 – Ball screw with servo motor (Lescoeur et al., 2017).....	24
Figure 2.15 – Hoisting system with stepper motors (Løken and Løkkevik, 2019).....	25
Figure 2.16 – Hoisting system with air cylinder (Akita et al., 2019).....	25
Figure 2.17 – Drilling system: 1– top drive, 2 – drill chuck, 3 – T-shaft, 4- azimuth motor, 5 – torque sensor, 6 – hydraulic swivel (Alvarez et al., 2022).....	26
Figure 2.18 – Steering system (Alvarez et al., 2022).....	26
Figure 2.19 – Oklahoma University rig’s top drive system (Akita et al., 2019).....	27
Figure 2.20 – Swivel and diverter (Alvarez et al., 2022).....	27
Figure 2.21 – Scheme of circulation system with two pumps (Khadisov et al., 2020).....	28
Figure 2.22 – Collecting box of the pneumatic circulation system (Løken and Løkkevik, 2019).....	28
Figure 3.1 – First version of MiniRig (Esmaili, 2013).....	31
Figure 3.2 – Current version of MiniRig	33
Figure 3.3 – MiniRig top drive	33
Figure 3.4 – Drilling console	34
Figure 3.5 – Page with drilling parameters	35
Figure 3.6 – Front and side views of the system.....	36
Figure 3.7 – Axonometric projection of the system.....	37
Figure 3.8 – Scheme of drill pipe connection	38
Figure 3.9 – Scheme of drill pipes breaking out	39
Figure 3.10 – Drilling wrench: a) model; b) kinematic scheme; 1 – hydraulic cylinder; 2 – cross beam; 3 – wedge plate; 4 – return spring; 5 – tangent wheel; 6 – follow-up roller, 7 – clamping arm,	40
Figure 4.1 – Speed pattern of the upper motor	42
Figure 4.2 – Torque pattern of the upper motor.....	44
Figure 4.3 – Speed pattern of the lower motor	46
Figure 4.4 – Torque pattern of the lower motor.....	49
Figure 4.5 – Gripping scheme (side view).....	51
Figure 4.6 – Gripping scheme (top view)	52
Figure 4.7 – Pipe with two grooves: a) axonometric projection; b) cross section of grooves .	53
Figure 4.8 – Latch mechanism.....	53
Figure 4.9 – Suspending scheme (top view).....	54
Figure 4.10 – Example of the electromechanical lock (Shenzhen YLI Electric Lock Co.,Ltd., 2014).....	55
Figure 4.11 – Pipe with four grooves: a) axonometric projection; b) cross section of grooves	56
Figure 4.12 – Eyemark optical sensor (Panasonic Electric Works SUNX Co., Ltd., 2011)....	57

Figure 4.13 – Phase shift principle of laser rangefinder (Wang et al., 2020)58
Figure 4.14 – Diagram of forces acting on the system (Sha et al., 2023)59

List of Tables

Table 4.1 – Results of moments of inertia calculation.....	43
Table 4.2 – Selected motor parameters	44
Table 4.3 – Results of moments of inertia calculation.....	47
Table 4.4 – Results of torque calculation.....	48
Table 4.5 – Features of different types of grippers’ drive sources.....	50
Table 4.6 – Calculation of the clamping force.....	59

Abbreviations

WOB	Weight on Bit
ROP	Rate of Penetration
PLC	Programmable Logical Controller
RPM	Revolutions per Minute